UNIVERSITY OF OKLAHOMA

GRADUATE COLLEGE

A COMPARISON OF POTENTIALLY IMPACT-RELATED DIAGENESIS IN IMPACT STRUCTURES WITH CARBONATE TARGETS

A THESIS

SUBMITTED TO THE GRADUATE FACULTY

In partial fulfillment of the requirements for the

Degree of

MASTER OF SCIENCE

By

EMILY N SIMPSON

Norman, Oklahoma

2021

Downloaded from SHAREOK. Persistent Handle URL: https://hdl.handle.net/11244/329499

A COMPARISON OF POTENTIALLY IMPACT-RELATED DIAGENESIS IN IMPACT STRUCTURES WITH CARBONATE TARGETS

A THESIS APPROVED FOR THE

SCHOOL OF GEOSCIENCES

BY THE COMMITTEE CONSISTING OF

Dr. R. Doug Elmore, Chair

Dr. Shannon Dulin

Dr. Michael Engel

© Copyright by EMILY SIMPSON 2021

All Rights Reserved.

Table of Contents

Acknowledgments---------- **v**

Abstract----------**vi**

1. Introduction----------**1**

2. Geologic setting/ sample location sites----------**5**

3. Methods----------**10**

4. Jeptha Knob

4.1. Results----------12

4.2. Discussion----------13

5. Serpent Mound

5.1 Results----------20

5.2. Discussion----------23

6. Decaturville

6.1. Results----------34

6.2. Discussion----------36

7. Isotope Results----------**44**

8. Discussion----------**47**

9. Conclusions----------**57**

10. References----------**58**

Acknowledgements

To start off, I would like to thank my advisor, Dr. Elmore. Thank you for taking me in as one of your students after I got here and for allowing me to be creative and really delve into my interests. You never shut down any of my ideas, but always helped to steer me in the right direction. Through your mentorship and professorship, I have grown and learned so much more about geology and myself and I will forever be grateful to have had such a fantastic advisor.

Next, I would like to thank my committee members Dr. Shannon Dulin and Dr. Michael Engel for taking the time to read and give me helpful comments and edits on my thesis. Your guidance and feedback were essential to the successful completion of my project. I also want to thank Dr. Dulin for her useful life advice over pizza that helped me to sort out some things regarding my long-term goals.

I am thankful to my fellow graduate students in Dr. Elmore's research group for the many things they taught me and for the thought-provoking questions they had along the way which enabled me to get a better understanding of my results. I also want to thank the other graduate students in my cohort for all of the great times we had together, I truly appreciate the friendship and support.

Lastly, I want to thank my family, specifically my parents, Patty and Rod Simpson for their amazing support. Neither of them had the means to attend college when they were my age and so I will be forever grateful for the sacrifices they have made to help me get here. I also very much appreciate the constant texting and calls with my mom, which made it seem as though I was not halfway across the country. I could not have done this without them.

Abstract

A petrographic and isotopic analysis of the carbonate target rocks at the Jeptha Knob structure, the Serpent Mound impact structure, and the Decaturville impact structure was conducted to better understand potentially impact-related diagenesis of carbonates.

Impact craters form during catastrophic events when objects from space hit the Earth's surface at high velocities and have high kinetic energy which is then partially transformed to thermal energy and leads the target rocks to experience high pressures and temperatures that deform them and can result in the initiation of a hydrothermal system (e.g.,Osinski et al., 2012).The goal of this study was to further the understanding of hydrothermal alteration related to the three relatively small complex impact craters in carbonate rocks, and to discuss the issues in distinguishing impact related diagenesis from other diagenetic events. The target rocks at two complex impact structures, Serpent Mound (Ohio), Decaturville (Missouri) and one probable impact, Jeptha Knob (Kentucky) were petrographically characterized regarding authigenic and hydrothermal phases present.

Paragenetic sequences were developed for all three structures and authigenic phases include pyrite, marcasite, hematite, magnetite, dedolomite, quartz, baroque dolomite, K-feldspar, biotite, and clays. Of these authigenic phases a number could be associated with hydrothermal deposits including marcasite, quartz, K-feldspar, biotite, clays, and baroque dolomite which have been reported as being common in post-impact hydrothermal systems (Osinski et al., 2012). Other evidence of hydrothermal activity, while not pervasive, includes veins filled with calcite and pyrite in some samples at Serpent Mound and Decaturville. It is difficult to distinguish between impact related hydrothermal fluids and other diagenetic events (e.g. orogenic fluids). Many of the authigenic minerals are localized to the impact structures suggesting they could be related to an impact-generated hydrothermal system, although the impact process could have produced fluid conduits for later diagenetic events. The results of this study suggest that hydrothermal alteration at small complex impact craters in carbonate target rocks can be identified but the alteration can be hard to distinguish from other diagenetic events.

1. Introduction

On Earth, there are nearly 200 confirmed impact craters. These formed during dramatic events when extraterrestrial objects hit the Earth's surface at high enough velocities to experience little deceleration as they pushed through the atmosphere (French, 1998). Some of these impact events were very destructive and led to mass extinctions (e.g. Chicxulub with the dinosaurs) and major changes in the Earth's climate. Features that are found at the hand sample and micro-scale are imperative for identifying a circular feature as an impact crater. These include shatter cones and shock metamorphic features within the minerals present (e.g. planar deformation features in silicates).

It has been shown that many impact events that are large enough to result in the formation of a complex impact crater will trigger a hydrothermal system (Osinski et al., 2012). Figure 1, from Osinski et al. (2012) shows where hydrothermal deposits are commonly expected within and surrounding a complex impact crater. On Earth, hydrothermal systems can form where there is a heat source and water present (Pirajno, 1992). This means that an impact (which can generate shock temperature substantial enough to melt large volumes of target rock) into a shallow-marine setting will provide the exact ingredients to generate a hydrothermal system (e.g. Zurcher and Kring, 2004; Osinski et al., 2012; Arp et al., 2013). While this is the case, the hydrothermal system that is generated will likely be relatively short-lived as the heat source will not remain for long after the impact event has occurred. In addition, it can be difficult to distinguish between impact related alteration by hydrothermal fluids and alteration by other diagenetic events such as orogenic fluids in relatively small impacts.

Paleomagnetism has been used to constrain the timing of alteration caused by the hydrothermal events because the flow of the hydrothermal fluids is hypothesized to create new magnetic minerals which record the magnetic field direction, essentially concurrently, with the timing of impact (e.g. Elmore and Dulin, 2007; Dulin and Elmore, 2008). These new minerals, which formed via the interactions between the host rock and the impact-generated hydrothermal fluids, can have interesting chemistries and the diagenetic effects can inform about the timing and longevity of the fluid flow as well as the composition of the fluid. Although many of the authigenic minerals are localized to the impact structures suggesting they could be related to an impact-

generated hydrothermal system, the impact process could have produced fluid conduits for later diagenetic events.

1.1 Hypotheses

Hydrothermal activity that is generated during the impact process has been documented in a number of terrestrial impact craters including Chicxulub in Mexico and the Reis crater in Germany (Zurcher and Kring, 2004; Arp et al., 2013; Osinski et al., 2004). The goal of this study is to further the understanding of alteration by impact-generated hydrothermal systems at three relatively small complex impact craters in carbonate rocks, and to discuss the issues in distinguishing impact related diagenesis from other diagenetic events. This will be done by studying the target rocks (carbonate units and impact breccia) at three impact craters in the US. These are the Jeptha Knob structure in Kentucky, the Serpent Mound impact structure in Ohio, and the Decaturville impact in Missouri.

The hypotheses to be tested are: 1. Impact-related hydrothermal alteration can be distinguished from other non-impact-related diagenetic events, and 2. The alteration observed will be localized to the impact structure and not found in the country rock outside of the structures.

1.2 Importance of this study

It is important to understand the age of impact structures and the effects that they have on the target rocks on Earth because this gives insights into the evolution of our solar system. For example, understanding large impacts that occurred after the time of the late heavy bombardment can give more information on what types of bodies were/are still floating around our solar system. It can also give us a better understanding of the causes of mass extinction events and paleoclimate following an impact event. Understanding the impact events on Earth can also aid in research of other bodies within our solar system (for example: Mars), which have experienced similar events throughout time. Characterizing the assemblage of diagenetic and hydrothermal minerals that formed at, or shortly after the timing of impact is also imperative for the use of paleomagnetism as a method for dating impact events.

Related to the two eastern structures (Serpent Mound and Jeptha Knob), there is evidence found in the eastern United States that regional fluid flow occurred due to secondary porosity in conduits within carbonate units and created late diagenetic dolomites (Montañez, 1997) that could

be similar to those found in Serpent Mound and Jeptha Knob. These pathways were likely opened as a result of the Alleghany orogeny which allowed for the migration of orogenic fluids (tectonic brines) through the country rock (Oliver, 1992) leading to the formation of new diagenetic minerals (Bethke and Marashak, 1990). It has also been suggested that these pathways for fluid migration remained open for later diagenetic events and hydrocarbon migration (Montañez, 1997). This project could provide more understanding on the spatial scale of the fluid flow following the Alleghany orogeny and could give insights into the economic importance of these structures.

Economic resources, specifically hydrocarbons and ore deposits, have been found in a number of impact structures on Earth. This includes around 12% of all impact structures on Earth having been exploited for their economic resources (Grieve and Masaitis, 2010). These economic deposits can form prior to impact and become redistributed because of the impact event, they can form during the impact as a result of the increased energy occurring and can lead to the formation of new phases, or they can form as a result of hydrothermal alteration which can cause fluid flow through the structure and potentially into structural traps formed during the impact (Grieve and Masaitis, 2010). The Ames impact structure located in Oklahoma, for example, is a complex impact structure with a 14km diameter that has been successfully exploited for hydrocarbons. The Arbuckle dolomite, a Lower Ordovician unit found in the area, does not have abundant porosity present, though as a result of fracturing and karstification during the impact, it has substantial economic value within the Ames structure (Grieve and Masaitis, 2010). It is possible that the Jeptha Knob, Serpent Mound, and Decaturville structures could also be potential hydrocarbon reservoirs as a result of impact-related faulting and fracturing and hydrothermal fluid alteration/migration into these carbonate-rich lithologies. It has also already been found at Decaturville that the sulfide deposits present, which were reworked during impact, could be exploited for their economic value (Grieve, 2005; Offield and Pohn, 1979).

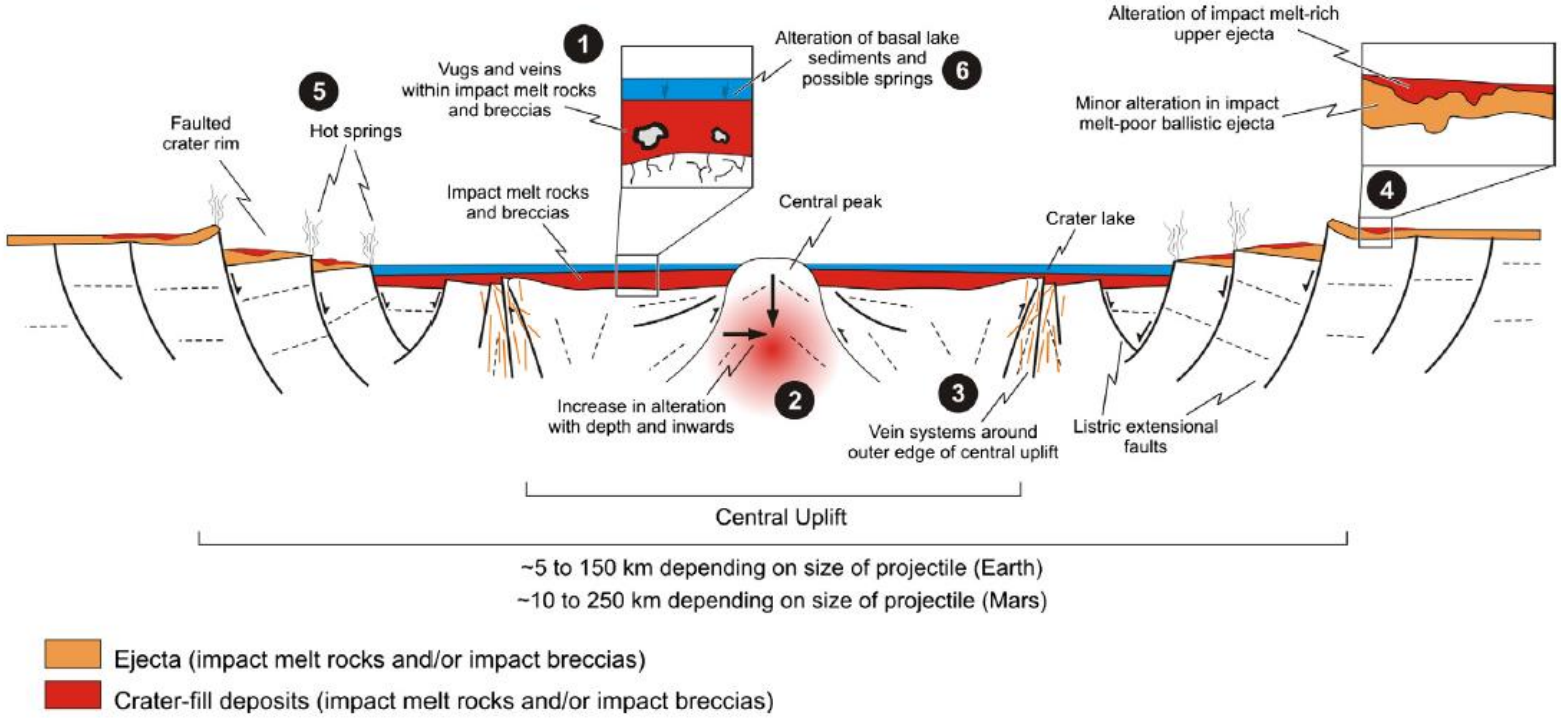


Figure 1: From Osinksi et al. (2012), showing the locations within and surrounding complex impact craters where hydrothermal deposits can be commonly found.

2. Geologic setting/ sample location sites

2.1 Background

Introduction to impacts

On Earth, impact craters form when an object from space penetrates the atmosphere without the loss of acceleration and then collides with the surface of the Earth (French, 1998). There are three stages that lead to the complete formation of an impact crater which can be seen in Figure 2: the first being the contact and compression stage, the second is the excavation stage, and the last stage to occur is the modification stage (French 1998). The contact and compression stage is the first interaction between the projectile and the target rock. The shock wave is initiated and begins to move through the target lasting on the order of a few seconds (French, 1998). During the excavation stage is when the transient crater forms due to the interactions between the propagating shock wave and the target ground surface, lasting up to a couple of minutes (French, 1998). Lastly, during the modification stage is when the transient crater begins to be affected by gravity, collapsing the rim and effecting the crater floor and having no real end (French, 1998). During these stages of formation, depending on the size and velocity of the projectile there are a number of different types of craters that can form. This thesis, as already indicated, will be focusing on the complex type of impact craters which are characterized by a centrally uplifted region surrounded by a relatively flat floor with a collapsed rim (Melosh 1989).

The ability to positively identify an impact crater relies not only on the recognition of a circular landform, but also on the identification of shock metamorphosed materials in the area within and surrounding the crater. When a shock wave travels through a target rock there is an immense pressure change that can lead to the permanent deformation of the crystal lattices in the minerals present in the target rocks. Different minerals respond differently because of their internal chemistry and crystal structures, as well as due to the unique geometry of the shock wave propagating ununiformly through the target (Langenhorst, 2002).

Introduction to shocked carbonates

Historically, silicates (and most specifically, quartz) have been the main focus of studies of shock metamorphism because they are the most abundant mineral found on Earth's surface (Clarke and Washington, 1924) and have thus been the target of more impacts. Silicates are

deformed by impacts in diagnostic ways and gain features that allows for the positive identification of impact structures (Langenhorst, 2002). While silicates are the most dominant mineral in Earth's crust, other minerals including carbonates have also been the target of many impacts, however they have not been the main focus of many impact studies, so generally less is known about them. The main deformational effects that carbonates experience during impact are not diagnostic of the impact process and can occur during regular tectonic events. These include mechanical twinning, lattice dislocations, and possibly CO_2 devolatilization (Burkhard, 1993; Hull and Bacon, 2001; Skala et al., 2000). Because of this, other methods, including changes in X-ray diffraction peaks, have been used to understand the deformation of the crystal lattice (e.g. Skala et al., 2000; Hanss et al., 1978; Bell et al., 1998; Fox, 2014; Simpson, 2019). This makes studying carbonate target rocks more difficult as the features in carbonates are not able to be definitively linked to an impact event. Also, because carbonates are much less stable than silicates and potentially experience decomposition during impact, they can acquire interesting diagenetic effects that are potentially related to and may be diagnostic of the impact event. Because of their non-diagnostic deformation, understanding the potentially diagnostic diagenetic effects to carbonates during impact is imperative for the study of impacts into carbonate targets. As previously discussed, these diagenetic components could play an important role in understanding the hydrothermal activity generated during impact and will be discussed for the following three structures.

2.2 Jeptha Knob

The Jeptha Knob structure (Fig. 3) is a probable complex impact structure with a diameter of around 4.25km located in Shelby County, Kentucky (Seeger, 1968).There is not clear evidence that this structure is an impact as no shatter cones, coesite, or PDFs have been observed at the surface (e.g. Cressman 1981), however supporting evidence for impact are a gravity study (Seeger, 1968), elevated levels of iridium (Seeger, 1968), and the X-ray Diffraction patterns of carbonates are consistent with other shock metamorphosed carbonates (Fox, 2014). The timing of the Jeptha Knob structure formation is constrained based on the units that have been deformed. The youngest unit deformed during impact is an Ordovician limestone that is capped by the undeformed, Silurian Brassfield Formation. There is a monolithologic breccia found within the central uplift that is similar to the breccias described at the Sierra Madera impact structure in Texas (Cressman, 1981).

2.3 Serpent Mound

The Serpent Mound impact structure is a complex impact structure located in Southwestern Ohio at the corner of Pike, Highland, and Adam's counties (Fig. 4). The diameter of the structure has not been well constrained because of subsequent erosion. Estimates range from 8km to 24km (Reidel et al., 1982; Milam, 2010; Vanadia, 2017). The evidence for this structure having been formed by an impact event comes from shock metamorphic effects seen in the minerals within and its overall morphology (e.g. Dietz, 1960; Reidel et al., 1982). The age constraints on Serpent Mound are poor and place the timing of impact between 330Ma and 256Ma based on a previous Paleomagnetic study done using only unoriented core (Watts, 2004). Further age constraints based on calcite twin orientations have narrowed the range down to 290-256Ma (Schedl, 2006). The main unit of focus in Serpent Mound is the Silurian Peebles Dolomite, and a secondary unit of focus related to the 2004 paleomagnetic study is the Silurian Brassfield Formation. Looking at the petrography of the Brassfield formation creates a link to the previous paleomagnetic study (Watts, 2004) and gives insights into what the magnetic mineralogy is and the formation mechanisms.

2.4 Decaturville

The Decaturville structure is a complex impact structure located in Southwestern Missouri and has a diameter of ~5.5km (Fig. 5). It is confirmed as an impact structure based on the identification of shatter cones as well as other shock metamorphosed features (Offield and Pohn, 1979). The age of this structure has not been well constrained because of its stratigraphy, although a paleomagnetic analysis found a magnetization that is younger than the impact breccia based on a conglomerate test and puts the younger age limit at Pennsylvanian-Permian (Dulin et al., 2007). The Ordovician Jefferson City Dolomite is the main unit of focus here and has been heavily brecciated within the structure due to the impact event. There is a sulfide breccia, containing Mississippi Valley Type sulfides found in the centrally uplifted area that will also be discussed. The type of breccias present here are similar to breccias reported at similar sized impact structures including Flynn Creek, TN and Sierra Madera, TX (Wilshire et al., 1971; Roddy, 1968).

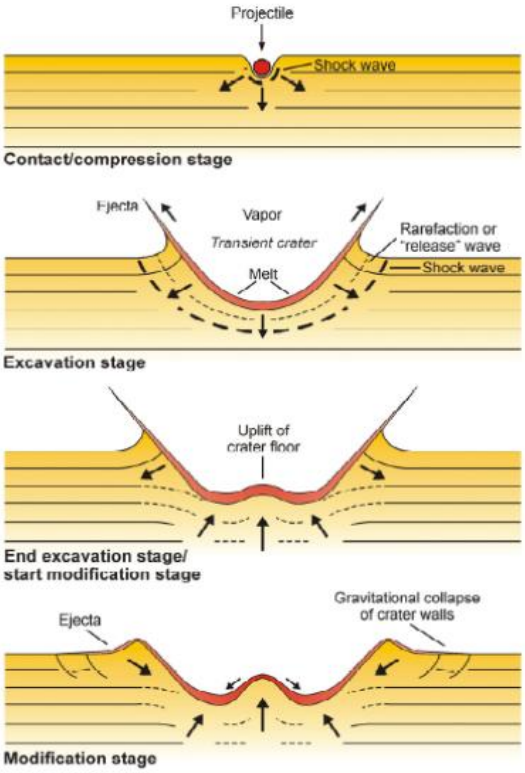


Figure 2: Detailing the formation of an impact crater from the initial contact and compression state through the final modification stage. Image from the Lunar and Planetary Science Institute. (https://www.psi.edu/epo/explorecraters/background.htm)

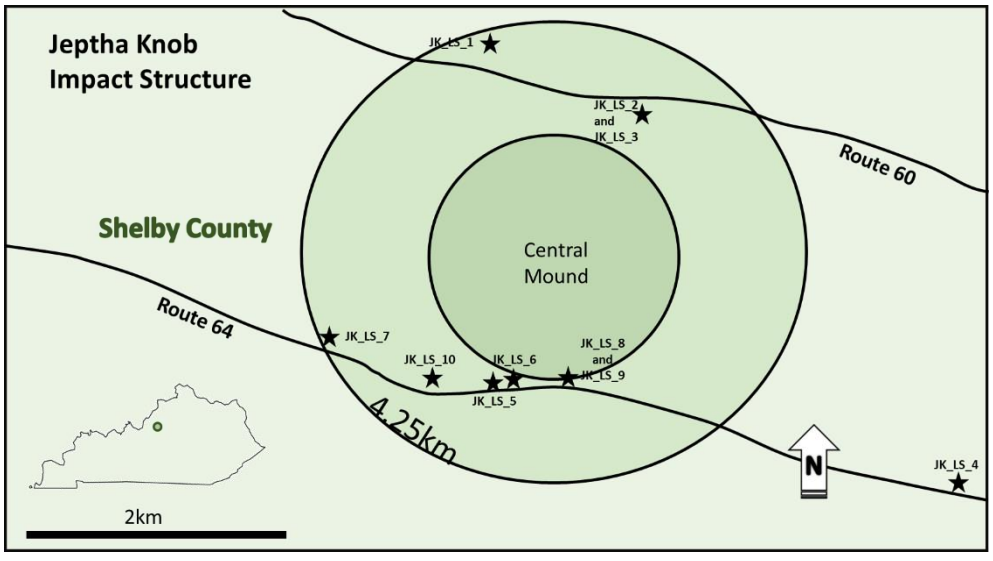


Figure 3: Map of the Jeptha Knob structure, northern Kentucky showing sample locations

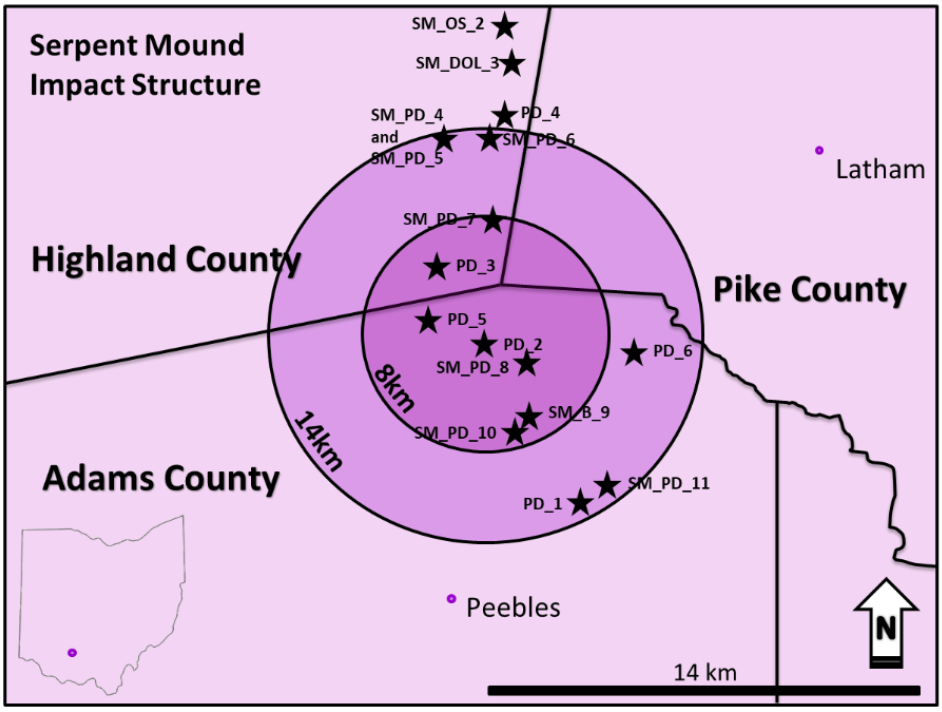


Figure 4: Map of Serpent Mound impact structure, southern Ohio showing sample locations

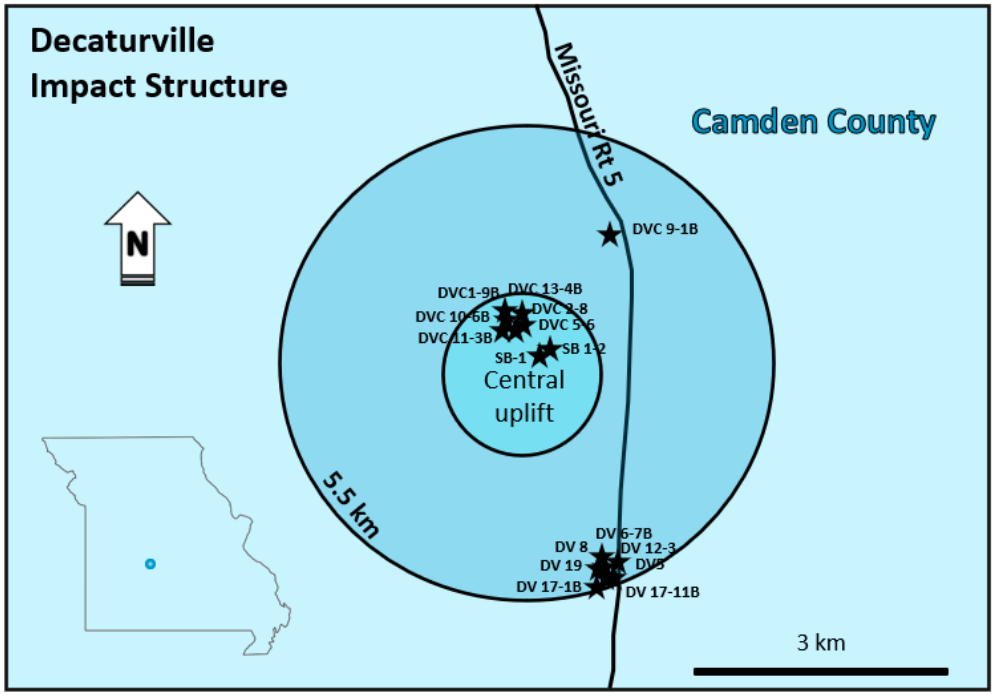


Figure 5: Map of the Decaturville structure, Missouri showing the sample locations

3. Methods

Within the three previously discussed structures, hand samples were collected from natural exposures and at Serpent Mound, a suite of samples were collected from cores drilled into the structure. The sample locations are shown in Figures 3, 4, and 5. Samples were collected from inside the structures, as well as a suite of samples from areas outside of the structures. At the Jeptha Knob structure, the main rock type is Ordovician limestone. Serpent Mound is an impact into a mixed target (containing both silicate and carbonate rocks) but the main focus here will be two Silurian carbonate units. The Decaturville structure has abundant impact-breccia and also a sulfide breccia found near the central peak.

At Jeptha Knob, samples were collected at the locations shown on the map in Figure 3. The amount of outcrop at Jeptha Knob was minimal and thus there were fewer samples able to be collected from this structure than the two others. However, a representative selection was collected, including a sample from outside of the structure for comparison. The samples that were collected from this structure include upper Ordovician limestone units.

At Serpent Mound samples were collected both from outcrops at the locations labeled on the map in Figure 4, as well as from five cores drilled into the structure and housed at the H.R. Collins Lab and Core Repository in Ohio. These are cores 2880, 2881, 2882, 3274, and 3275 drilled into the northern rim (2880, 2881, and 2882), central uplift (3274), and western transition area (3275). The formation that was focused on in outcrop was the Upper Silurian Peebles Dolomite and the formation of focus in the cores was the Lower Silurian Brassfield Formation.

At Decaturville the sample location sites can be seen in Figure 5. The main units that were collected include monomict and mixed breccias. These were both collected from a large outcrop along the southern edge of the structure ~2km from the central uplift. Within the central part of the structure mixed breccias were the main unit collected, and a number of these samples came from a pile of cores found near the center of the crater. Samples of the Jefferson City Dolomite (which makes up the monomict breccia and is found as clasts in the mixed breccia) were collected from outside of the structure for comparison.

Standard polished thin sections were produced from the samples in order to identify the minerals present and to develop paragenetic sequences for the impacted rocks. Petrographic

analysis was done using the Zeiss Axio Imager.Z1m microscope. This analysis was done in order to understand the mineralogy and observe the fabrics present. After having identified interesting features in the thin sections, they were then analyzed using the FEI Quanta 250 scanning electron microscope (SEM) fitted with a Bruker XFlash 6I100 energy dispersive spectroscopy (EDS) attachment in order to identify the elements present in the samples. The SEM system was operating at an accelerating voltage typically at 20kV, but from a range between 15kV to 25kV with a spot size of 5µm and a working distance of 10mm. Using this combination of the Zeiss microscope and the SEM allowed for a thorough understanding of the mineralogy and for the development of a paragenetic sequence for each structure.

Stable isotopic analysis was done on the samples from all three impacts. This included carbon and oxygen isotopes. The analysis was done at the Utah State University Stable Isotope Laboratory and included obtaining the carbon and oxygen isotopic signatures for approximately 30 samples (10 from each structure). The samples were prepared by sealed tube reaction of the carbonate with phosphoric acid (H_3PO_4) at 50°C and then the oxygen isotope ratios of the dolomite-rich samples were corrected to 25°C. Some of the samples were not purely calcite or dolomite and contained a small amount of the other mineral. However, the abundance of the other mineral in the samples was minimal and they were oxygen corrected assuming either 100% dolomite or 100% calcite depending on the sample. The isotope abundances are reported in delta notation with parts per thousand relative to the PeeDee Belemnite (PDB) standard. Carbon and oxygen isotopes give insights into devolatilization of calcite and dolomite during impact because it has been documented that volatilized CO_2 has quite different C and O isotopic ratios than the initial carbonate (Martinez et al., 1994). Because of the relatively rapid effects that occur during impact, it is unlikely that thermodynamic isotope equilibrium can occur, however kinetic fractionation is possible, and typically results in more negative isotopic ratios in the product, and heavier isotopes in the remaining carbonate (Martinez et al., 1994). This analysis was done in order to understand any potential devolatilization that may have occurred and to better understand the extent and origin of hydrothermal fluid alteration related to impact. Carbonates that have experienced hydrothermal alteration via externally derived fluids typically have carbon isotope ratios of < -4‰ (VPDB) and oxygen isotope ratios of > 10‰ (VSMOW) (e.g. Hecht et al., 1998; Zheng and Hoefs, 1992; Spangenberg et al., 1996) however, these values will be heavily dependent on the fluid's isotopic value.

4. Jeptha Knob

4.1 Results and Interpretations

Petrography

The samples from Jeptha Knob include the Upper Ordovician Calloway Creek Limestone and the Grant Lake Limestone. The Calloway Creek and the Grant Lake Limestones are both fossiliferous limestones with minor interbedded shale. Because of the similarity between these two formations, they are grouped together here and are simply referred to as fossiliferous Ordovician limestone. Using Dunham's classification of carbonate rocks, these would be considered packstones to grainstones dominated by bryozoans and brachiopods.

Diagenetic features observed in the samples from within the structure include pyrite (both framboidal and cubic), stylolites, dolomite, dedolomite, and possible hydrothermal minerals similar to those discussed by Osinski et al. (2012), including quartz, anatase, K-feldspar, biotite, and clay minerals (most likely illite based on energy dispersive analysis and fabric). Calcite twinning is observed in all of the samples from within the crater, however very minimal twinning is observed in sample JK-4 from outside of the crater. Because of the relative lack of calcite twinning outside of the structure, it is thought that the twinning present here was likely formed during the impact. The uplift of the Cincinnati arch began in the Middle Ordovician (Borella and Osborne, 1978) and continued to form during the deposition of the units discussed here, so it is possible that this deformation could have also contributed to the formation of the twins in the calcite observed.

Figure 6a shows a photomicrograph of the fossiliferous limestone in the structure crosscut by a highly serrated to deformed stylolite. Stylolites are common throughout all of the samples from Jeptha Knob. In the samples from the southern half of the structure though, these stylolites are always associated with dolomite and dedolomite (Figure 6b), whereas in the northern half of the structure minimal dolomite was identified. The rest of the rock from the southern half does not contain many dolomite grains, so much of the dolomite appears to have formed along the stylolites but is not dissolved by the stylolites, suggesting that the paragenesis of the dolomite occurred during or after stylolitization. In the instances where dolomite grains are found in the samples not associated with stylolites, many appear to be baroque dolomite (Figure 6c) exhibiting the

characteristic curved grain boundaries and undulatory extinction. Calcite overgrowths on fossils are also common as is shown in Figure 6d.

Scanning Electron Microscopy

A number of the samples from Jeptha Knob that had interesting features, like stylolites, dedolomite, and baroque dolomite when observed in the petrographic microscope, were also observed using the SEM. Figure 7a shows dedolomite which occurs when Ca-rich fluids enter the system and from the weathering and release of iron from Fe-dolomite (Von Morlot, 1847 as cited by Schoenherr et al., 2018) thereby replacing the existing dolomite rhombs with calcite and precipitating hematite (from the excess Fe).

As previously mentioned, pyrite is common and found both as pyrite framboids and as cubic pyrite. In Figure 7b it can be observed that both forms of pyrite are being partially replaced by iron oxide (likely hematite). This SEM image shows cubes of pyrite with rims of FeO forming, as well as partially and completely replaced framboids. Figure 8a shows more altered pyrite framboids and cubes which are now almost entirely FeO. This figure also shows an abundance of clays (likely illite because of the flakey, ribbon-like fabric) along a stylolite. In Figure 8b anatase associated with quartz is observed and clays infilling pore space can be seen. Anatase is not common in these rocks, but when observed is always found in association with quartz grains and is typically confined to infilled pores. This figure also shows that the dolomite grains present in these samples are commonly ferroan based on energy dispersive analysis. Figure 8c shows a pore within a sample that is infilled with dolomite, minor pyrite, and authigenic K-feldspar and biotite.

4.2 Discussion

A paragenetic sequence of the rocks at Jeptha Knob can be seen in Figure 9. This shows the relative timing of the formation of the different diagenetic phases observed with those that are potentially related to impact highlighted in red. The earliest diagenetic phase is thought to be calcite cement (e.g., Fig. 6d) which would likely form during early burial. As compaction continued, stylolites formed early in the diagenesis of these rocks as well, and as previously discussed, much of the dolomite is found associated with stylolites indicating its formation occurred after the stylolites. As discussed above, pyrite is observed both as framboids and as cubic crystals. The pyrite framboids are thought to occur during relatively early diagenesis and, while

previously thought to form via the replacement of greigite by pyrite, are now thought to form via the reaction of amorphous iron monosulphide and aqueous hydrogen sulfide without the intermediate greigite being necessary (Butler and Rickard, 2000). The cubic form of the diagenetic pyrite is thought to form later in the paragenetic sequence based on its presence associated with other later features and in infilled pores. It has been found that the amount of supersaturation in a system and the growth temperature have a large effect on hydrothermally grown pyrite grains, and in order to grow a cubic pyrite crystal, the system has to have a higher degree of supersaturation and temperatures near or above 250°C (Murowchick and Barnes, 1987), though cubic pyrite can also form non-hydrothermally. Dedolomite formed later in diagenesis as Ca-rich fluids entered the system and replaced dolomite with calcite and led to hematite formation from the excess Fe in the system. Late in the paragenetic sequence hematite is also observed replacing earlier pyrite framboids and cubes (Fig 7b).

The clay minerals present could have formed relatively early but are thought to possibly have a second occurrence that formed during late diagenesis. Two occurrences of clay minerals is thought to be because of the presence of clays along stylolites (which are thought to have formed early in the diagenetic history of these samples), and then also infilling pore space (which is thought to have formed as a result of dedolomitization during middle diagenesis). Quartz and anatase are found together with quartz typically lining pores and anatase found within them. Baroque dolomite formed later than the other dolomite in the diagenetic sequence and was likely the result of the flow of moderate to high-temperature hypersaline brines (Warren, 2000) possibly related to impact. Some of the last phases thought to have formed diagenetically are K-feldspar and biotite, both likely hydrothermal.

A number of these phases could be related to hydrothermal activity occurring within the structure, possibly soon after the impact. Baroque dolomite is formed via precipitation from hydrothermal brines, typically at temperatures above 150°C (Scholle and Ulmer-Scholle, 2003) and is not observed in the sample from outside of the structure. Authigenic quartz is commonly found in the early high-temperature stages of hydrothermal alteration and is prevalent in complex impact craters (Osinski et al., 2012). Primary anatase is also found in impact-related hydrothermally altered rocks (Osinski et al., 2012). Hydrothermal K-feldspar is another silicate mineral found in impact craters (Osinski et al., 2012). Biotite is also found in samples from inside

of Jeptha Knob and is possibly related to post-impact hydrothermal activity leading to the alteration of silicates and forming hydrated silicate phases like the clays observed (Osinski et al., 2012), although based on fluid inclusion data, the temperatures experienced may not have been high enough here to produce hydrothermal biotite. JK-4, collected from outside of the structure, is not observed to contain any of these potentially hydrothermal phases, providing further evidence for the phases having formed as a result of the impact and not as a result of a regional event.

The best evidence for a hydrothermal system having been active in this structure is the presence of baroque dolomite and authigenic biotite. The other phases discussed above, while commonly found as hydrothermal minerals in complex impact structures, are also found in other diagenetic environments and are not diagnostic of a hydrothermal setting (e.g. Waugh, 1978 on authigenic K-feldspar). It is also possible that the baroque dolomite and the other potentially hydrothermal phases could be younger than the impact. This would indicate that later diagenetic fluids flowed through these rocks and filled the porosity created by the impact. It is difficult to distinguish between impact related diagenetic features with other diagenetic events, specifically in this setting where many of the phases present are also found in carbonate units that have not experienced an impact. While this is true, the results presented here are consistent with what is reported by Schedl and Seabolt (2016) at Jeptha Knob including hydrothermal dolomite which contains fluid inclusions with formation temperatures of 85-115°C, hydrothermal quartz, and euhedral pyrite all of which are interpreted to have formed as a result of the impact (Schedl and Seabolt, 2016). The hydrothermal nature of the quartz could also explain why no shocked quartz has been identified within the structure, because it would have formed directly following impact.

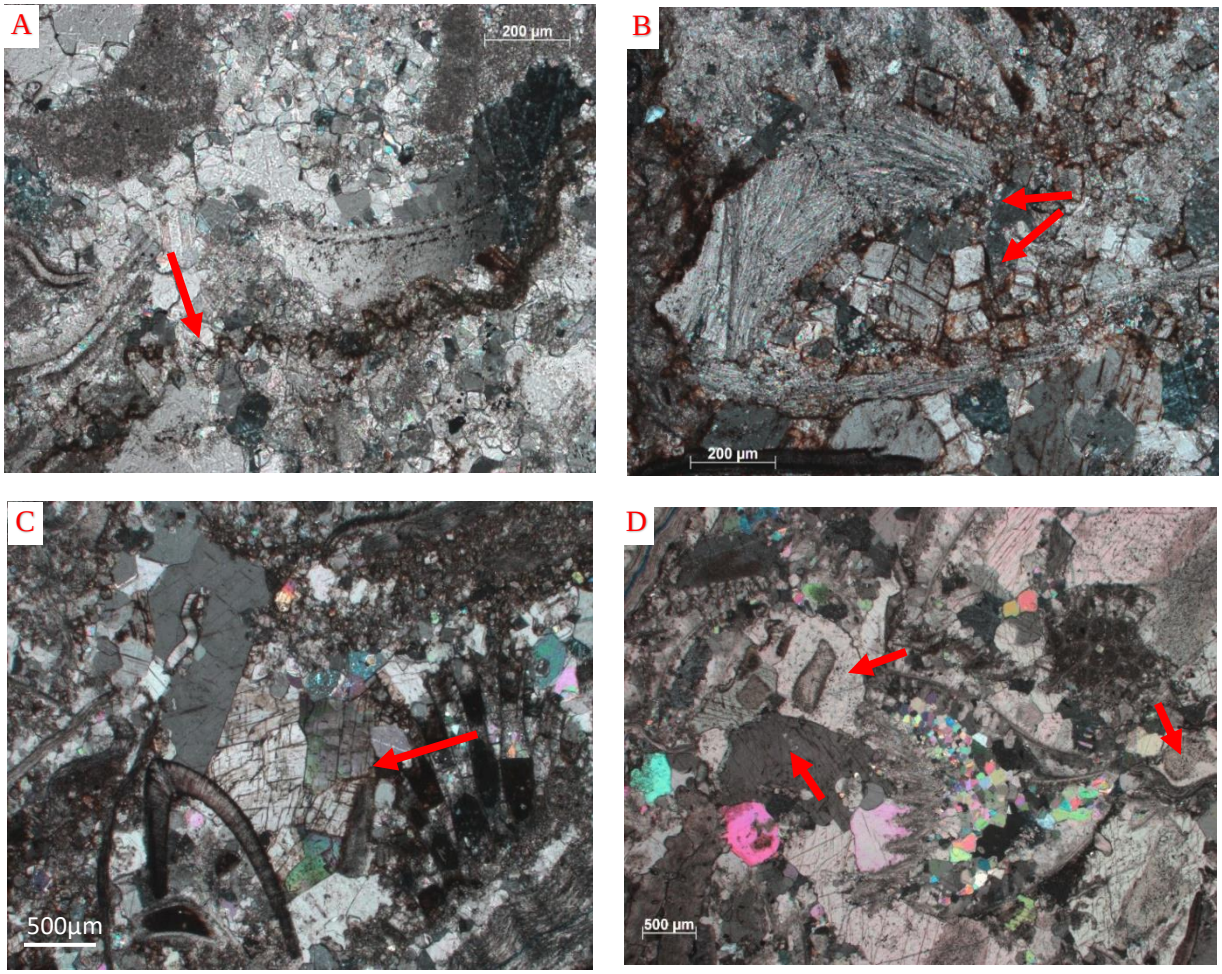


Figure 6: Photomicrographs of samples from Jeptha Knob, all in XPL, (A) JK-1 from the northern half of the Jeptha Knob structure showing a fossiliferous Ordovician limestone containing a highly serrated to deformed stylolite (indicated by the arrow); (B) JK-8 from the southern half of Jeptha Knob showing dedolomite (dolomite rhombs partially taken over by hematite and calcite indicated by an arrow) associated with a stylolite along the boundary of a fossil (also indicated by an arrow); (C) JK-8 showing baroque dolomite grains (arrow) in the center with curved grain boundaries and undulatory extinction; (D) Photomicrograph showing calcite overgrowths on echinoderm fossils (arrows).

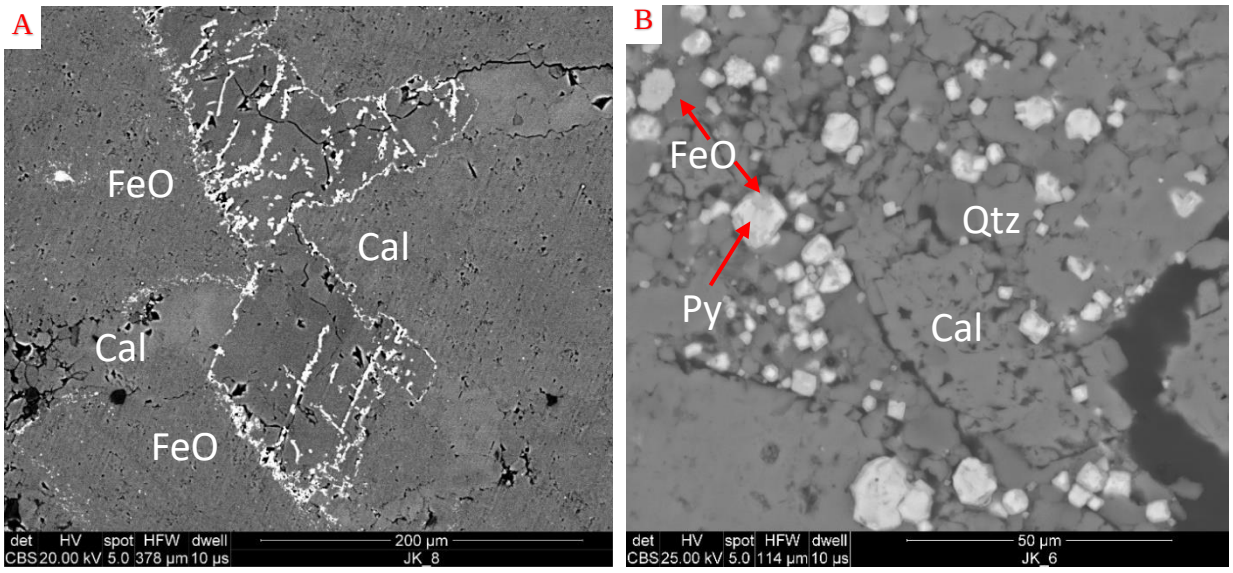


Figure 7: (A) Backscatter SEM image of sample JK-8 showing dedolomite with hematite having formed in the growth zones of the dolomite crystals which have been replace by calcite; (B) Backscatter SEM image of sample JK-6 showing pyrite (both framboidal and cubic) being replaced by FeO (likely hematite).

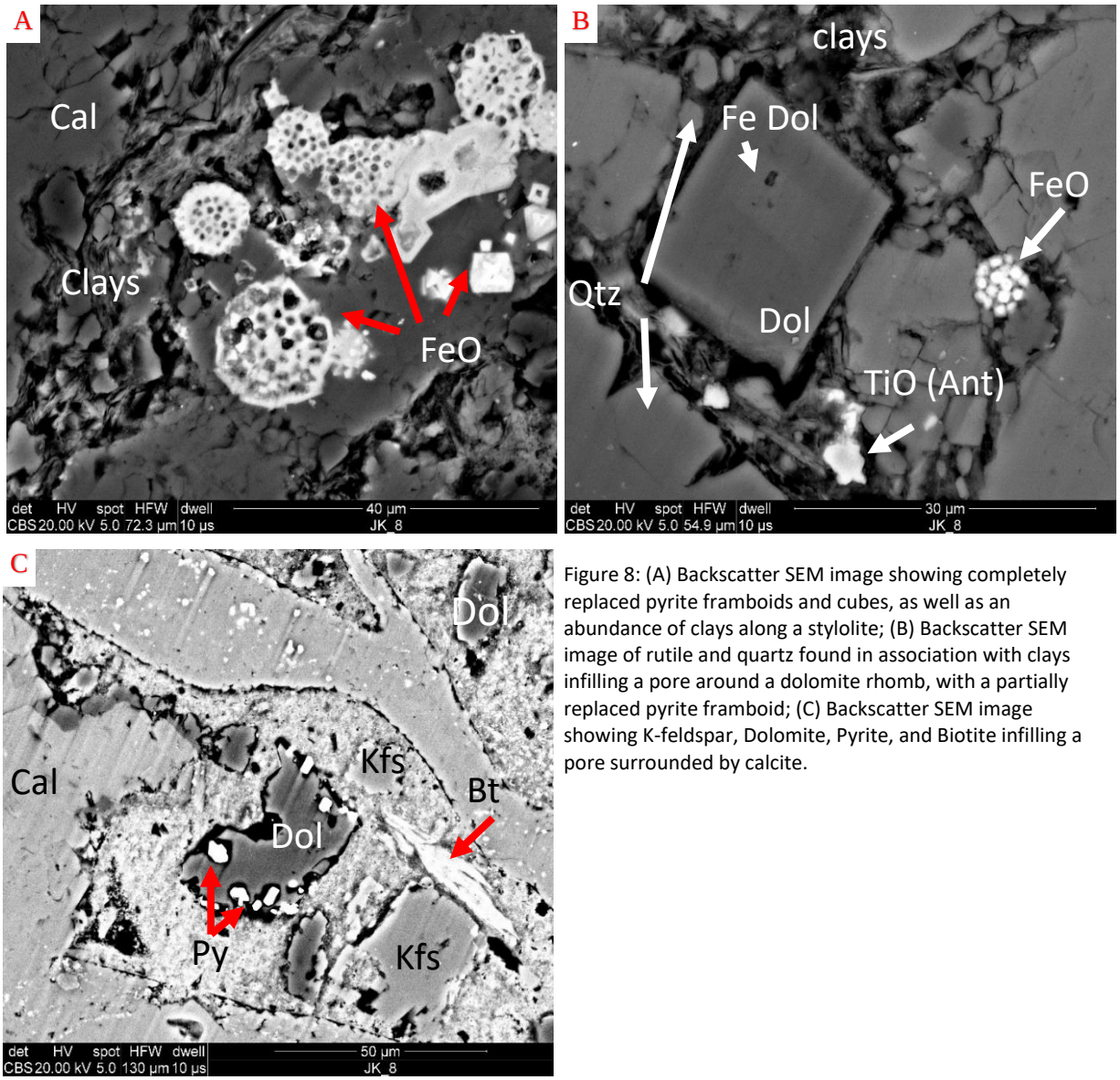


Figure 8: (A) Backscatter SEM image showing completely replaced pyrite framboids and cubes, as well as an abundance of clays along a stylolite; (B) Backscatter SEM image of rutile and quartz found in association with clays infilling a pore around a dolomite rhomb, with a partially replaced pyrite framboid; (C) Backscatter SEM image showing K-feldspar, Dolomite, Pyrite, and Biotite infilling a pore surrounded by calcite.

Diagenetic Phases	Relative timing Early	Middle	Late
Calcite cement	--------		
Stylolitization	----------		
Dolomite	----------		
Pyrite framboids	------	----------	
Dedolomite (Hematite + Calcite)		----------	
Porosity		----------	
Pyrite (cubic)		----------	------
Hematite (replacing pyrite)			----------
Clays	----------		----------
Quartz			----------
Anatase			----------
Baroque Dolomite			----------
K-feldspar			----------
Biotite			----------

Figure 9: A paragenetic sequence of the diagenetic phases present at Jeptha Knob showing the relative timing of authigenesis. Phases highlighted in red are thought to be related to an impact-generated hydrothermal system.

5. Serpent Mound

5.1 Results and Interpretations

Petrography

Peebles Dolomite

The Peebles Dolomite is a Middle-Upper Silurian dolostone unit that is generally a thickly bedded crystalline dolomite with replaced fossils. The fossil molds are typically of stromatoporoids, corals, bivalves, and gastropods; stromatoporoids being the most common (Kahle, 1988). The dolomite crystals are non-ferroan and typically subhedral-euhedral and cloudy, sometimes with dark cores suggesting they formed in a mixing-zone environment (Kyser et al., 2002). The Peebles dolomite has been split into three informal members: the upper Serpent Mound Breccia (SMB), the middle Vuggy member, and the lower Blue member (Milam et al., 2010; Simpson, 2019). The samples discussed here are primarily the SMB and the vuggy member. The SMB is not an impact breccia. It was formed during the Middle-Late Silurian and represents highly eroded Peebles Dolomite that was deposited prior to the impact (Milam et al., 2010). Further analysis is needed to know the mechanism for brecciation/deposition (Milam et al., 2010) though it is possible it is a paleokarst feature that caused *in situ* brecciation which is found in the northern equivalent to the Peebles Dolomite, the Lockport Dolomite (Kahle, 1988).

Diagenetic features in the Peebles include stylolites, dolomite, vugs/porosity, quartz, anatase, K-feldspar, minimal clay, and sulfide minerals. Asphaltic material is also common in the Peebles in the area of Serpent Mound (Baranoski et al., 2003). It appears that the migration of this material occurred prior to the impact and is likely linked to the migration of fluids out of the Appalachian Basin and into the study area which occurred during the late Alleghany Orogeny (Baranoski et al., 2003; McCabe and Elmore, 1989). As discussed for Jeptha Knob, a number of the diagenetic phases present could indicate hydrothermal activity, for example, the quartz, anatase and sulfides (Osinski et al., 2012). Overall, the Peebles Dolomite does not contain abundant diagenetic features other than two dolomite types, as described below, vugs, and stylolites, which are very common.

Figure 10a, a sample from the northern rim of the structure, shows the characteristic subhedral-euhedral and cloudy dolomite rhombs (Type 1) of the Peebles Dolomite. This is a sample of the informal vuggy member and the abundant porosity is observed. Through the center

of the photomicrograph a stylolite is present. Stylolites are identified throughout the structure and are common within the Peebles. Figure 10b is another sample of the Peebles with euhedral dolomite rhombs (Type 1) that have dark/cloudy cores. This sample has most of its pore space infilled with lath/tabular shaped dolomite crystals (Type 2) that are clear (Figure 10b and c) and lack the cloudy appearance of the other dolomite type. This dolomite is present in a number of the samples and is typical of evaporitic conditions and its presence in the pores of these samples suggests it formed later in the paragenetic sequence than type 1 dolomite as environmental conditions were changing from marine to marine-evaporitic conditions and its growth occurred within existing porosity (e.g., Gillhaus et al., 2010). The presence of two dolomite types indicates two dolomitization events. The first dolomitization event was very early in the diagenesis of the Peebles, and the second was later, remobilizing Ca and Mg during evaporitic conditions and crystalizing dolomite in existing pore space.

Brassfield Formation

The Brassfield Formation is a Lower Silurian limestone unit found across northern Kentucky, Ohio, and eastern Indiana. It is composed of interbedded shales, limestones, dolomite, and, what will be focused on here, hematitic limestone. Similar to the Peebles, it experienced two dolomitization events. The first was focused in the Belfast Member (supratidal environment producing cloudy, anhedral crystals), and the second was regional dolomitization which was a later diagenetic event interpreted to be related to a mixing zone environment close to the Cincinnati arch (Varga, 1981). This hematitic limestone forms the upper contact of the Brassfield Formation in the area around Serpent Mound. Hematite is commonly found in the Brassfield and other Silurian aged units in the surrounding states, however this hematite-rich layer is generally restricted to the area surrounding Serpent Mound. The abundance of hematite here is related to the initial stages of uplift of the Cincinnati arch creating a relatively oxic environment during deposition due to increased circulation in the shallow marine setting (Oakley, 2013).

Diagenetic features observed in the Brassfield are similar to those discussed in the Peebles Dolomite and include the two generations of dolomite (the first within allochems and lithic clasts (Type 1, Fig. 13a), the second in the groundmass (Type 2, Fig. 11d)). Hematite cement, calcite cement, dedolomite, and hematite associated with the dedolomite are common features. Stylolites are not common in the Brassfield as they are in the Peebles. Sulfide minerals, while relatively

common in the Peebles, are not common in the Brassfield and only a small amount of pyrite is observed.

Figure 11a shows a sample of the Brassfield Formation from the central uplift of the structure. This sample is the only outcrop sample of Brassfield discussed here; the rest of the samples are from five cores drilled into the structure. In the photomicrograph an abundance of calcite twinning can be observed. This twinning is thought to have been a result of the deformation caused during impact (Schedl, 2006) as this sample is from the most deformed part of the structure. In Figure 11b, the same sample of the Brassfield is shown with a large fracture that is infilled with calcite. This calcite is substantially less twinned than what is seen in Figure 11a suggesting it infilled the fracture after the deformation caused by the impact. Dedolomite was identified in this sample and prompted further collection of samples of the Brassfield in order to better understand the dedolomite and its relationship to the previous paleomagnetic study done on the cores. Figure 11c shows a sample from core 2880 in the northern rim/ transition area of the crater. This sample contains a lithic clast with ferroan zoned dolomite rhombs that have been partially dedolomitized with hematite forming around them. There is a clear truncation line surrounding this grain that cross cuts dolomite crystals and is annotated with a red dashed line. This sample also contains an abundance of allochems that have been partially to entirely replaced by hematite. Figure 11d is a closer view of the hematite replaced allochems that are very common in the Brassfield samples; this sample also contains dedolomite in the left half of the slide.

Scanning Electron Microscopy

Figure 12a shows an SEM image of a sample from the northern rim of the structure. This shows that in the Peebles dolomite, sulfide minerals are relatively common and specifically here pyrite can be seen with acicular marcasite needles growing on the edges of the pyrite grain. Pyrite framboids are more common than cubic pyrite and are often observed being replaced by FeO. In Figure 12b, an SEM image, a sample from near the central uplift is shown and a grain of authigenic anatase can be seen in association with quartz. Figure 12c shows a vug that is infilled with K-feldspar, clays (likely kaolinite based on the fabric and EDS analysis), quartz, and FeO. Figure 12d contains a crystal of monazite found in the Brassfield formation. Only 1 crystal of monazite was identified so it is not thought to be common in Serpent Mound.

A close-up of the hematite-replaced allochems in the Brassfield formation can be seen in Figure 13a. This figure also contains an allochem with a large, zoned dolomite crystal that is truncated by a hematite rim. Another notable feature in this image is contact hematite cement identified between allochems. Figure 13b, an SEM image, shows the same lithic clast as Figure 10e. In the SEM, the zoning of the dolomite rhombs can be better seen, and the hematite can be seen replacing dolomite grains. The truncation around this clast is clearer here as well, and some hematite can also be seen forming a slight rim around the clast. Hematite-rich allochems are found in the matrix surrounding this clast. A different kind of hematite-rich allochem can be seen in Figure 13c, which shows hematite ooids with calcite cement between. The presence of ooids indicates that these likely precipitated as hematite, rather than replacing already present allochems like those previously discussed. Both the replaced allochems and the hematite ooids are thought to be predepositional and were incorporated into the Brassfield during its formation. Variations in the color of layers forming the ooids can also be seen in Figure 13d where Al, Si, and Fe were mapped and indicates that the darker layers are less iron-rich and contain more aluminum and silica. This is likely the clay mineral chamosite, which has been reported in other hematite ooids (Young, 1989).

5.2 Discussion

As mentioned above, there are a number of diagenetic features present in the rocks at Serpent Mound. Paragenetic sequences of the Peebles and the Brassfield can be seen in Figures 14 and 15, respectively. A combined paragenetic sequence for Serpent Mound is shown in Figure 16. The earliest feature is thought to be dolomite, as there were early dolomitization events that occurred in both the Peebles and the Brassfield. Other early features include vugs/porosity, stylolites, asphaltic material, apatite, and pyrite framboids. The abundant porosity and vugs are thought to have formed very early in the diagenesis of the Peebles related to subaerial exposure and paleokarst activity. They were likely forming prior to/ during the deposition of the overlying Greenfield Formation (Kahle, 1988). Contact hematite cement and calcite cement are found in the Brassfield and are both thought to be syndepositional/ early diagenetic features. Quartz and anatase are found adjacent to pore space in the Peebles. A dedolomitization event occurred in the Brassfield after the second dolomitization event that formed ferroan dolomite. This likely occurred during middle diagenesis and led to the formation of more calcite and hematite. Cubic pyrite formed later

in the diagenetic history and, in the Peebles, was subsequently followed by a second generation of hematite formation as the pyrite framboids and cubes were partially replaced by hematite. A second dolomitization event occurred in the Peebles infilling pore space with lath/tabular shaped dolomite grains. K-feldspar and clays are uncommon but where they are present are generally found infilling pore space in the Peebles. Marcasite is found growing on pyrite cubes and is thought to have formed due to the remobilization of sulfides that likely occurred during the impact. Monazite was also identified in the sample of the Brassfield collected at the surface and is thought to have occurred relatively late, but the exact timing is unsure as there was only one crystal found and there were no cross-cutting relationships to aid in placing it in the sequence.

In southwestern Ohio, sulfide mineralization is localized to the Serpent Mound structure (Botoman and Stieglitz, 1978). The sulfide minerals are commonly found in the Ordovician, Silurian, and Devonian limestones and dolostones within the structure (Heyl and Brock, 1962; Reidel, 1972). The most common sulfide minerals are pyrite, marcasite, and sphalerite, the first two were identified in this study within the Peebles dolomite. Within Serpent Mound, faults cross-cut sphalerite and are also healed by sphalerite indicating that its formation occurred prior to and following impact (Schedl, 2006). This indicates that there were sulfides present prior to the impact (these being Mississippi Valley Type sulfide deposits), that were then likely remobilized after the impact leading to the sphalerite healing the faults and also the marcasite as discussed above. There are also fluid inclusions present within the sphalerite grains that indicate temperatures of 85-180°C during the impact (Schedl, 2006). The presence of these fluid inclusions could be further evidence suggesting hydrothermal activity following impact.

Along with the marcasite needles and the sphalerite indicating remobilization of sulfides related to impact and hydrothermal activity, a number of the other diagenetic phases could also be related to hydrothermal activity following impact. These include the quartz, anatase, K-feldspar, clays, and monazite. Quartz, anatase, K -feldspar, and clays, as discussed with Jeptha Knob, are commonly found in complex impact structures that experienced hydrothermal activity following impact (Osinski et al., 2012). These minerals are not necessarily diagnostic of hydrothermal settings though, so it is possible their formation was under other diagenetic conditions. Monazite is another phase present here that is possibly hydrothermal in origin and related to the impact. Monazite is a common metamorphic mineral and is also found in hydrothermally-influenced

carbonate sedimentary rocks (Overstreet, 1967). It is thought that at Serpent Mound the monazite identified likely formed due to the hydrothermal system generated during the impact, though it is not a common phase found in these rocks.

A previous paleomagnetic study was done on Serpent Mound and focused on the hematite-rich intervals of the Brassfield Formation. This study found two magnetic components, one giving a Modern age and one giving an age of Late Permian/ Early Triassic (Watts, 2004). As discussed above, in the samples of the hematite-rich Brassfield collected adjacent to where paleomagnetic samples had been collected, there appears to be three occurrences of hematite. The first being the allochems that had been almost entirely replaced by hematite which are interpreted to have formed prior to deposition as evidenced by the cross-cutting relationships with dolomite crystals and the clear truncation lines surrounding the grains (Figure 13a and b). The hematite ooids are also thought to be predepositional and were incorporated into the Brassfield during its formation. The second and third occurrences are hematite cement between allochems and dedolomite. The allochems are possibly the remnants of an eroded condensed zone that then eroded and redeposited the hematite-rich allochems and hematite ooids in the Brassfield during its formation in the Early Silurian when the area was experiencing a marine transgression followed by a regression (Brett et al., 1990).

Modern iron-rich ooids are rare. However, there is evidence that indicates their formation can be related to hydrothermal fluids traveling through seafloor sediments, which allows for an increase in iron and silica in the system (Di Bella et al., 2019). This process could explain the banded hematite-chamosite ooids present within the Brassfield formation. The presence of the hematite ooids and the potential for them having formed via hydrothermal fluid interactions indicates that during the deposition of the Brassfield formation, it is possible that there was a hydrothermal system active in the area of the Serpent Mound structure, though this would be much earlier than the formation of the structure itself and therefore not related to impact. The Brassfield formation is Early Silurian, whereas the Peebles Dolomite is Middle-Upper Silurian, so this pre-impact hydrothermal influence cannot account for the potentially hydrothermal phases present within the Peebles as it was not yet deposited.

An interesting and puzzling aspect of the paleomagnetic results from the Brassfield is that the hematite that has replaced the allochems and forms the ooids, which are abundant, was

predepositional based on the petrographic relationships discussed above. One would expect this to carry an early magnetization as opposed to a Permian remagnetization. For example, a study of the Cambrian Morgan Creek Limestone in central Texas found a Cambrian magnetization in hematite that was interpreted to be associated with allochems replaced by hematite as well as a Modern remagnetization, also residing in hematite, that is associated with modern dedolomite (Loucks and Elmore, 1986). The reason there is not a Silurian magnetization is puzzling but could be because the magnetization in the replaced allochems was randomized during deposition.

There is also some hematite cement between the hematite replaced allochems (Figure 13a). The timing of this hematite postdates the hematite in the allochems but the timing compared to the dedolomite hematite is unknown. It could have been soon after deposition or much later. It is possible that it could carry the Permian remagnetization. The Permian timing of the remagnetization is consistent with the remagnetization event that affected a large area of the North American craton during the Kiaman reversed epoch (Watts, 2004).

Another genesis of hematite in this formation is in the form of dedolomite that can be a near-surface diagenetic event indicating it is the cause of the Modern age (Loucks and Elmore, 1986) or it could be due to Ca-rich fluids, perhaps derived from evaporites. This would indicate that the timing of the dedolomite formation could be similar to the lath/tabular shaped dolomite forming under evaporitic conditions. This would have been possible during the late Permian/ Early Triassic as southern Ohio, as evidenced by the Permian aged rocks deposited in SE Ohio/ NW West Virginia, was experiencing periodic evaporitic conditions (Martin, 1998). Dedolomite formation during the Permian when Ohio was experiencing these periodic evaporitic conditions could explain the late Permian/Early Triassic magnetization found in these rocks but does not explain the lack of earlier magnetization.

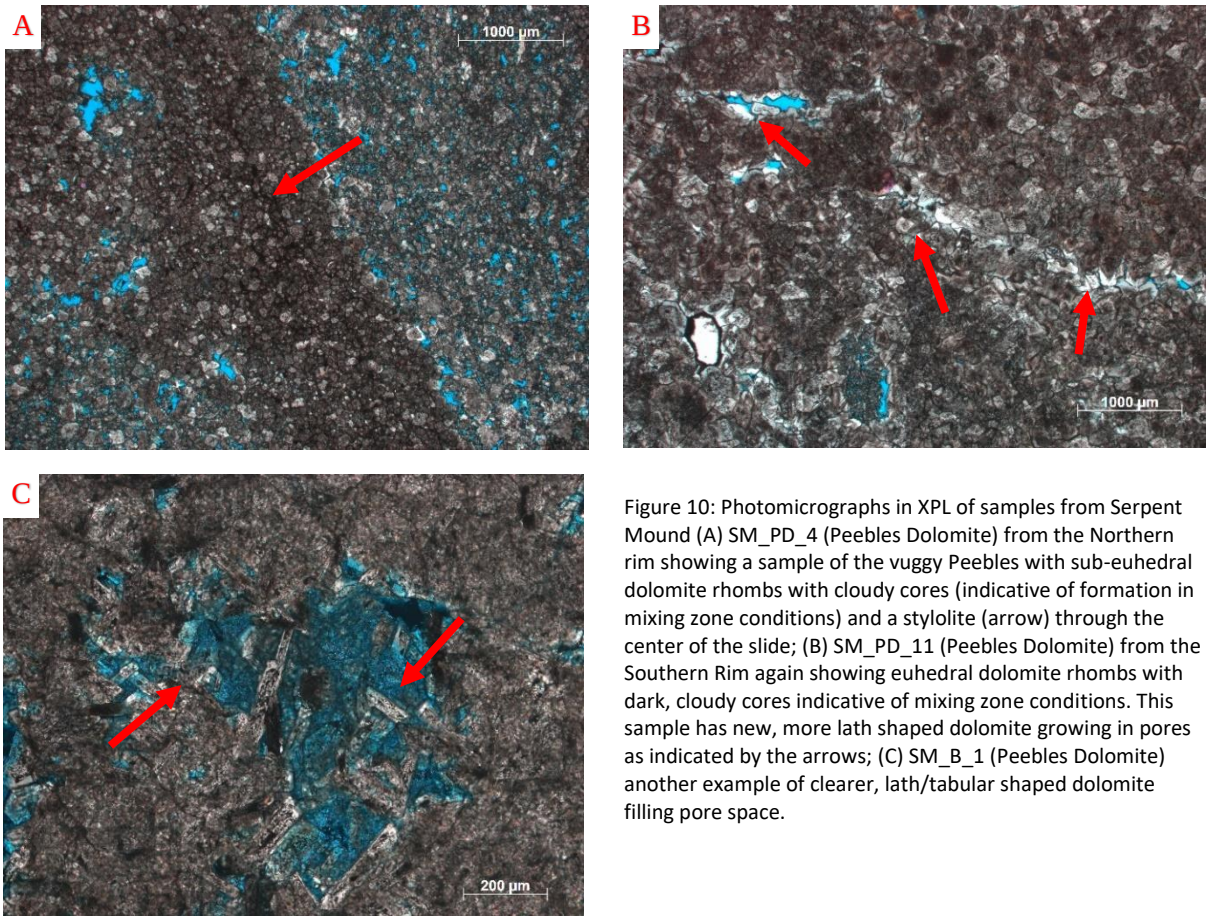


Figure 10: Photomicrographs in XPL of samples from Serpent Mound (A) SM_PD_4 (Peebles Dolomite) from the Northern rim showing a sample of the vuggy Peebles with sub-euhedral dolomite rhombs with cloudy cores (indicative of formation in mixing zone conditions) and a stylolite (arrow) through the center of the slide; (B) SM_PD_11 (Peebles Dolomite) from the Southern Rim again showing euhedral dolomite rhombs with dark, cloudy cores indicative of mixing zone conditions. This sample has new, more lath shaped dolomite growing in pores as indicated by the arrows; (C) SM_B_1 (Peebles Dolomite) another example of clearer, lath/tabular shaped dolomite filling pore space.

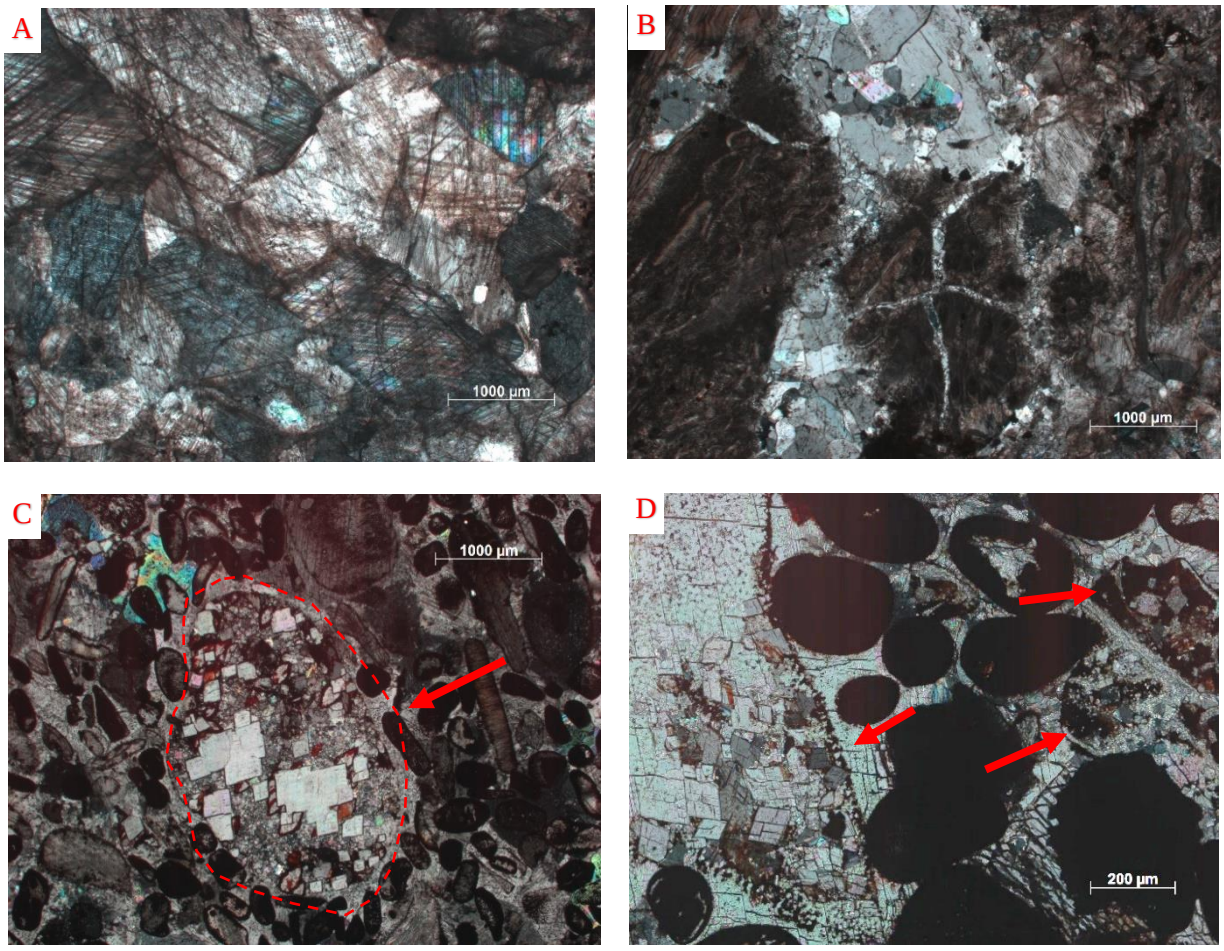


Figure 11: (A) PD_2 (Brassfield Formation) from the central uplift (only sample of the Brassfield formation from outcrop) showing heavily twinned calcite grains that were deformed during the impact; (B) PD_2 (Brassfield Formation) again from the central uplift showing a fracture infilled with calcite that is substantially less twinned than what is seen in (A) indicating it formed after impact; (C) 2880 BFH_1 (Brassfield Formation) from a core in the North transition area showing a lithic clast (arrow and dashed line) with euhedral dolomite grains and numerous allochems replaced by hematite; (D) 2880 BFH_3 (Brassfield Formation) showing hematite replaced allochems and dedolomite (arrows).

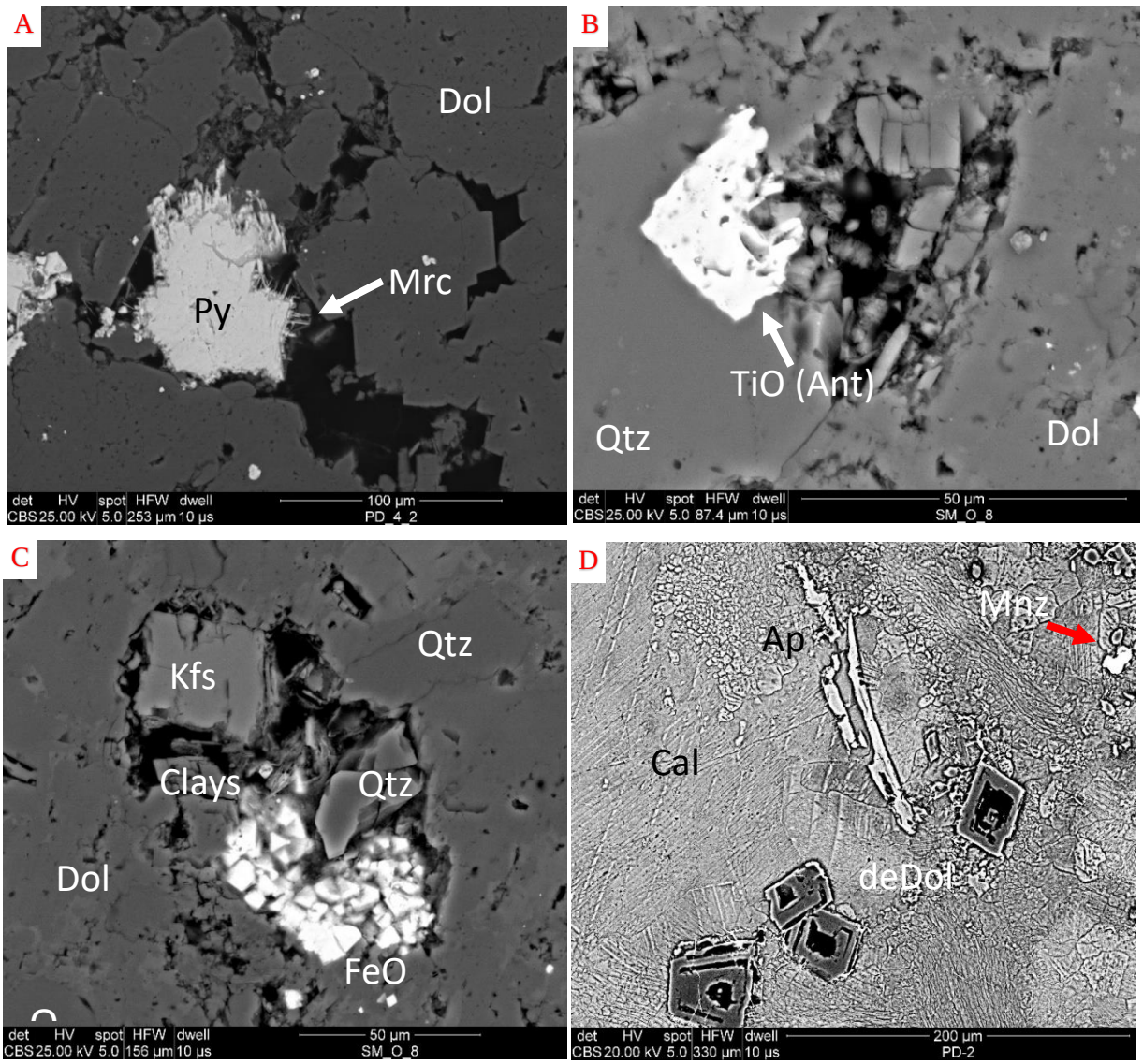


Figure 12: (A) Backscatter SEM image of PD_4 from the northern rim of Serpent Mound showing a pyrite grain with acicular marcasite growing on the edges; (B) Backscatter SEM image of SM_PD_8 showing a grain of authigenic anatase surrounded by quartz; (C) Backscatter SEM image of SM_PD_8 showing K-feldspar, clays, quartz, and FeO infilling a vug in the Peebles; (D) Sample PD_2 of the Brassfield formation from the central uplift containing apatite, dedolomite, and a crystal of monazite.

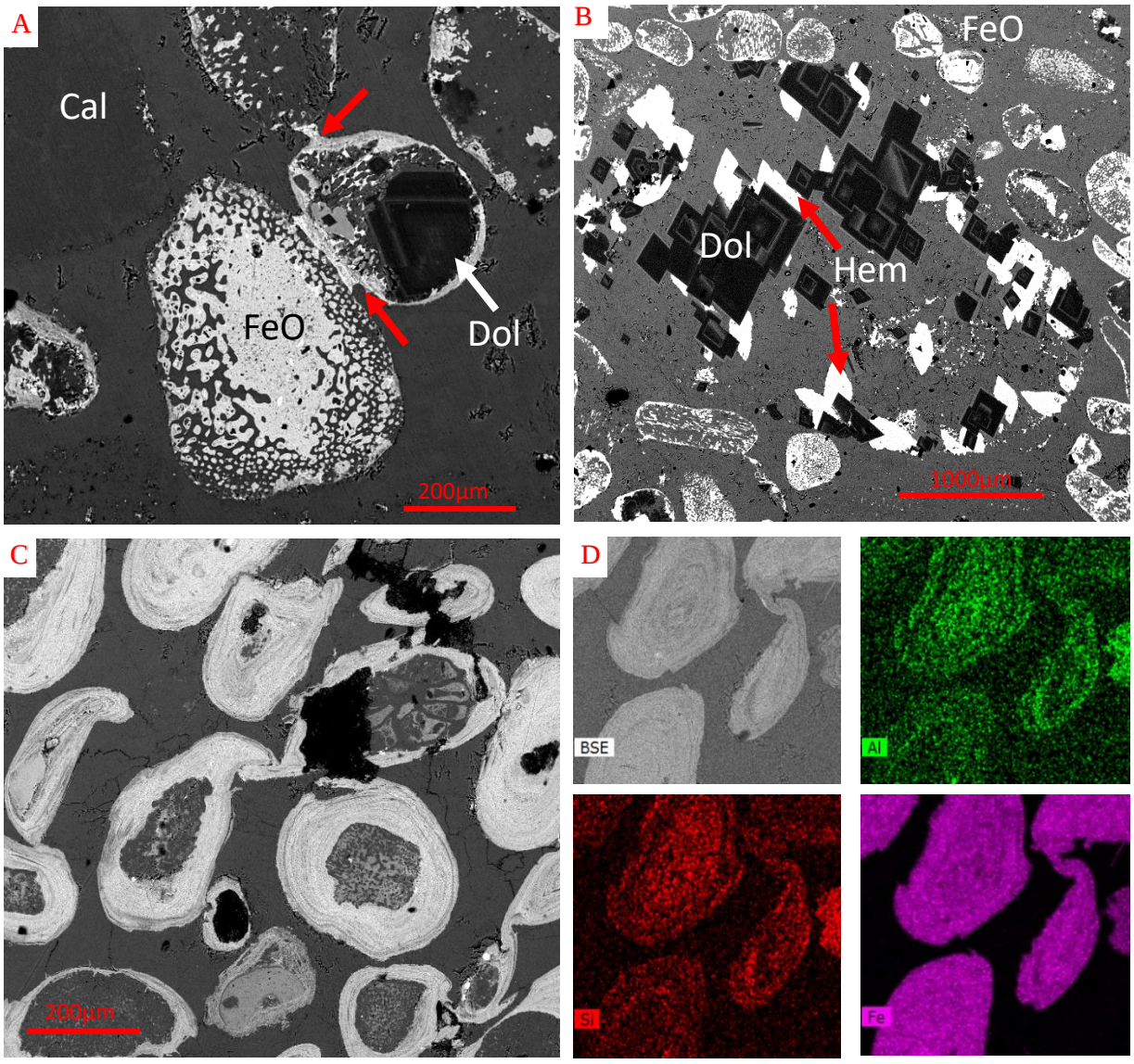


Figure 13: (A) Backscatter SEM image of 2880 BFH_1 from the northern transition area of the structure showing an allochem entirely replaced by hematite with another allochem that has a large, zoned dolomite crystal truncated by a hematite rim, contact cement indicated by arrow; (B) Backscatter SEM image of 2880 BFH_1 showing a lithic clast with zoned dolomite rhombs surrounded by hematite, with hematite-rich allochems in the matrix; (C) Backscatter SEM image of 3275 BFH_2 showing more hematite-rich allochems, these ones appear to be zoned hematite indicating they are ooids and could have precipitated as hematite, rather than being replaced like the others; (D) Backscatter SEM image with Al, Si, and Fe mapped to show the differences in the darker layers in the ooids, which based on the elements present, appear to be chamosite.

Diagenetic Phases Peebles Dolomite	Relative timing Early	Middle	Late
Dolomite	----------		
Paleokarst features (molds, vugs)	----------		
Stylolites	----------		
Asphaltic material	----------		
Pyrite (framboids)	----------		
Quartz	----------	----------	
Anatase		----------	
Pyrite (cubic)		----------	----------
Sphalerite (as indicated in the literature)		----------	----------
FeO (replaced pyrite framboids and cubes)			----------
Lath/tabular dolomite			----------
K-feldspar			----------
Clays			----------
Marcasite			----------

Figure 14: Paragenetic sequence of the Peebles Dolomite in the Serpent Mound structure showing the relative timing of formation of the diagenetic phases.

Diagenetic Phases Brassfield Formation	Relative timing Early	Middle	Late
Dolomite rhombs within allochems/lithic clasts	----------		
Hematite-replacing allochems	----------		
Contact hematite cement	----------		
Calcite cement	----------		
Apatite	----------		
Dolomite	----------	------	
FeO (hematite dedolomite)		----------	
Pyrite (cubic) (very minimal)			----------
Monazite			----------
Calcite infilling fractures			----------

Figure 15: Paragenetic sequence for the Brassfield formation found within Serpent Mound showing the relative timing of formation of the diagenetic phases. The two features highlighted in red are thought to have occurred prior to deposition and were included within the hematite-rich section of the Brassfield. The feature listed in grey is thought to have occurred post-impact.

Diagenetic Phases	Relative timing Early	Middle	Late
Dolomite rhombs within allochems/lithic Clasts (Type 1 Brassfield)	----------		
Dolomite (Type 1 Peebles)	----------		
Paleokarst features (molds, vugs)	----------		
Hematite-replacing allochems	----------		
Stylolites	----------		
Asphaltic material	----------		
Contact hematite cement	----------		
Calcite cement	----------		
Apatite	----------		
Dolomite (Type 2 Brassfield)	----------	-----	
Pyrite (framboids)	----------		
Quartz	----------	----------	
Anatase		----------	
FeO (hematite dedolomite)		----------	
Pyrite (cubic)		----------	----------
Sphalerite (as indicated in the literature)		----------	----------
FeO (replaced pyrite framboids and cubes)			----------
Lath/tabular dolomite (Type 2 Peebles)			----------
K-feldspar			----------
Clays			----------
Marcasite			----------
Monazite			----------

Figure 16: Combined paragenetic sequence for both the Peebles Dolomite and the Brassfield Formation showing the relative timing of formation for the diagenetic phases present within the Serpent Mound impact structure.

6. Decaturville

6.1 Results and Interpretations

Petrography

The samples from Decaturville are primarily breccias. There are two main breccia types present in the area of the structure, a monomict breccia and a mixed breccia. The mixed breccia is the dominant rock type present in outcrop in the center of the structure and is found associated with faults (Offield and Pohn, 1979). The monomict breccia's occurrence is due to brecciation within single beds and does not have multiple lithologies, nor is it associated with fault traces (Offield and Pohn, 1979). This unit includes the fine-medium grained crystalline dolostone of the Ordovician Jefferson City Dolomite. Mississippi Valley Type sulfide deposits are common in these rocks, specifically in the center of the structure, however they are not thought to have formed during the impact, as cross-cutting relationships indicate they were present before impact (Zimmerman and Amstutz, 1972). Samples from the center of the structure will be discussed here, as well as samples from an outcrop approximately 2km south of the center that was the focus of a previous paleomagnetic study (Dulin and Elmore, 2008).

Center Samples

Diagenetic phases present in the samples from the central part of the Decaturville structure include dolomite, sulfide minerals, and K-feldspar. Figure 17a shows a large clast in a mixed breccia sample from the central part of the structure that contains large ferroan dolomite rhombs with zoned outer rims and dark/cloudy cores. This is common of the dolomite observed in most of the samples here, and is indicative of formation in fluctuating mixing zone, marine conditions (Kyser et al., 2002). Sulfide minerals observed in the mixed breccia samples from the central part of the structure include galena, sphalerite, and pyrite. Unlike the two other structures discussed, no framboidal pyrite is observed. Only cubic pyrite is present. Figure 17b shows a breccia sample with clasts of opaque galena and pyrite cubes in the matrix with a large dolostone rock fragment on the right edge of the slide.

Southern Samples

Diagenetic phases present in the samples 2km south of the center of Decaturville include dolomite, hematite, anatase, dedolomite, and K-feldspar. Figure 17c is a sample of the mixed breccia, showing the fine-grained matrix with a vein running through it. The components of the matrix here include dominantly dolomite, with minor amounts of quartz, calcite, and some small clasts. The vein contains much coarser grained dolomite that is being replaced by calcite and hematite as it is dedolomitized. Figure 17d is another sample from the southern outcrop showing a large clast of dolostone with dolomite rhombs (formed prior to impact) that have cloudy cores and opaque grains (hematite). Figures 17e and f is a sample of a mixed breccia from the southern outcrop that shows the matrix which contains vugs infilled with baroque dolomite. The curved grain boundaries and undulatory extinction are present in many of the crystals within these vugs. This provides evidence of a possible impact-related hydrothermal system that led to hydrothermal fluid migration following brecciation. Baroque dolomite was not identified in the samples from outside of the structure, providing further evidence for its formation having been impact-related.

Scanning Electron Microscopy

Center Samples

Following analysis on the petrographic microscope, samples were analyzed in the SEM to further understand fabrics observed and the phases present. As previously mentioned, galena, pyrite and sphalerite are common in some of the mixed breccia samples from the center of the structure. Figure 18a shows a large cube of galena surrounded by dolomite and pyrite in the matrix of a breccia sample. It is interpreted as a detrital fragment incorporated in the breccia. There is a mineral also present within the matrix in this sample (Figure 18b) that contains arsenic based on energy dispersive analysis. This is galena that has inclusions of As. Some of the grains are very irregular, elongated, and appear too fragile (Fig. 18b) to have survived brecciation. They do not appear to be detrital and are interpreted as authigenic. This mineral is relatively common in the sulfide-rich breccia from the central part of the structure (Figure 18b) and often has rims of cerussite. This phase, in contrast to the inclusion-free galena, is interpreted as post brecciation. Figure 18c is another example of this type of grain with a similar fabric and it also has a cerussite rim. This picture also contains a number of sphalerite grains, which are common, and have pure zinc rims. Figure 18d shows another cube of galena. This one contains a cerussite rim and has a texture that appears to be the result of slight dissolution along the grain boundaries. The original

grains of galena and sphalerite are likely detrital, but the rims are thought to be post brecciation. In Figure 19a, the galena has inclusions of arsenic along growth plains and in 19b an intergrowth of galena and sphalerite can be seen. This intergrowth is likely pre-brecciation and impact (Zimmerman and Amstutz, 1972), although the zinc rim present on the sphalerite is probably post depositional (and therefore post-impact).

Southern Samples

Based on SEM analysis, authigenic K-feldspar is common in these samples. In Figure 20a, K-feldspar grains can be seen associated with dolomite and hematite in a breccia clast. Quartz grains are also commonly found in association with K-feldspar in these samples. The K-feldspar grain on the left appears to have an overgrowth on it indicating the grain itself could be detrital but may have a post-brecciation authigenic component. Authigenic anatase is also present as can be seen in Figure 20b of a small clast within the matrix (Fig. 17c). The relationship of the grains in this image is interesting and appears to show the replacement of dolomite by calcite and formation of some hematite. The anatase also has inclusions of dolomite (Figure 20b) within it, indicating its formation having been at a similar timing, but likely prior to the dedolomitization event. Figure 19c shows another sample from the southern outcrop that contains hematite-replaced pyrite (as indicated by the cubic shape) that is beginning to be replaced by another iron oxide, interpreted as magnetite. Grains of hematite being replaced by magnetite can also be seen in Figure 20d.

6.2 Discussion

A paragenetic sequence for Decaturville can be seen in Figure 21. This shows the relative timing of the formation of the detrital and authigenic phases present in these rocks. Pre impact events include one dolomitization event. The deposition of the Mississippi Valley Type sulfide deposits (sphalerite, galena, and pyrite) was also pre-impact as previously discussed. Authigenic quartz grains are also thought to have formed early in the diagenetic history of these samples and was likely not related to the impact.

Anatase is present and, as mentioned above, formed after the dolomite, and likely prior to dedolomitization because of the inclusions of dolomite grains within the anatase (Figure 20b). Dedolomite is relatively common in these samples and a second generation of hematite could be related to release of Fe during dedolomitization (e.g., Elmore et al., 1985). During the

dedolomitization process and the mobilization of cations, it is common for porosity to increase. It is thought that vugs formed at a similar timing to dedolomitization. The baroque dolomite is interpreted to have formed via hydrothermal fluid migration (Scholle and Ulmer-Scholle, 2003) and occurs in vugs in the matrix of the breccia suggesting that it is post impact. K-feldspar, as is consistent with what was observed at Jeptha Knob and Serpent Mound, possibly formed relatively late in the paragenetic sequence, and could be related to the impact-generated hydrothermal fluids. However, at Decaturville it is more difficult to distinguish if it formed pre or post brecciation based on textural evidence. Of the samples collected from further outside of the crater, none contain any of the hydrothermal or potentially hydrothermal phases. This is consistent with the interpretation that possible hydrothermal phases formed as a result of the impact and not as a result of a regional event.

The sulfides, as discussed above, are Mississippi valley type lead zinc deposits and are not related to the impact event. According to Zimmermann and Amstutz, (1972), these sulfides were crystallized in the host rock before brecciation and movement occurred. This indicates a hydrothermal system unrelated to the impact event taking place prior to impact and leading to the formation of the sulfide minerals. This does not fully explain the unusual shapes of the galena with As inclusions, or the cerussite rims around the grains which are probably post depositional. According to Leach et al. (2010) when MVT deposit material has a fracture system, atmospheric oxygen can reach As-bearing sulfides like sphalerite or pyrite and release the As which can then become incorporated into other minerals. With a relative abundance of pyrite, sphalerite, and galena present in the MVT deposits that were present prior to impact, it is possible that when the impact-related fracture systems were opened and a post impact hydrothermal system was activated, the galena with As inclusions formed. It is known that the galena was formed pre brecciation (as was indicated in Zimmerman and Amstutz, 1972) and then was incorporated into the breccia during impact. The PbAsS however, is thought to be post impact because of its authigenic fabric and because of the cerussite rims and is likely related to the remobilization of sulfides after the impact. Occurring at similar timing to this, the partial dissolution of sphalerite leaving zinc rims on many of the grains provides further evidence for remobilization during/directly following impact. These remobilized sulfides along with the baroque dolomite provide the best evidence for diagenesis related to the impact event.

Later events which could be pre or post impact include hematite replacing pyrite. Following hematite formation, magnetite replaced some of the hematite (Figure 20c and d) as well as some pyrite. The magnetite is clearly authigenic. Based on the paleomagnetic study (Elmore and Dulin, 2007), breccia clasts at the southern outcrop contain a chemical remanent magnetization (CRM) residing in magnetite that failed a conglomerate test and was post depositional. The pole position indicates the CRM formed in the early Permian. Away from the impact to the south, the Jefferson City Dolomite contains an older Pennsylvanian magnetization. Previous paleomagnetic studies of carbonate units which contain a CRM and magnetite replacement of pyrite, indicate that the magnetite formed at low temperatures (e.g., Elmore et al., 2012). Conodonts from the breccia indicates a CAI index of ~1 which suggests a temperature of about 100ºC which is too low for hydrothermal fluids. However, as discussed above there are a number of phases present that indicate a hydrothermal system was active at the time of impact. The reason the conodonts do not indicate hydrothermal temperatures could be because the temporal scale of impact-related hydrothermal systems is likely very short and would not have had a long enough duration to alter the conodonts. This previous paleomagnetic analysis indicated that the magnetization provides a young limit on the age of the impact.

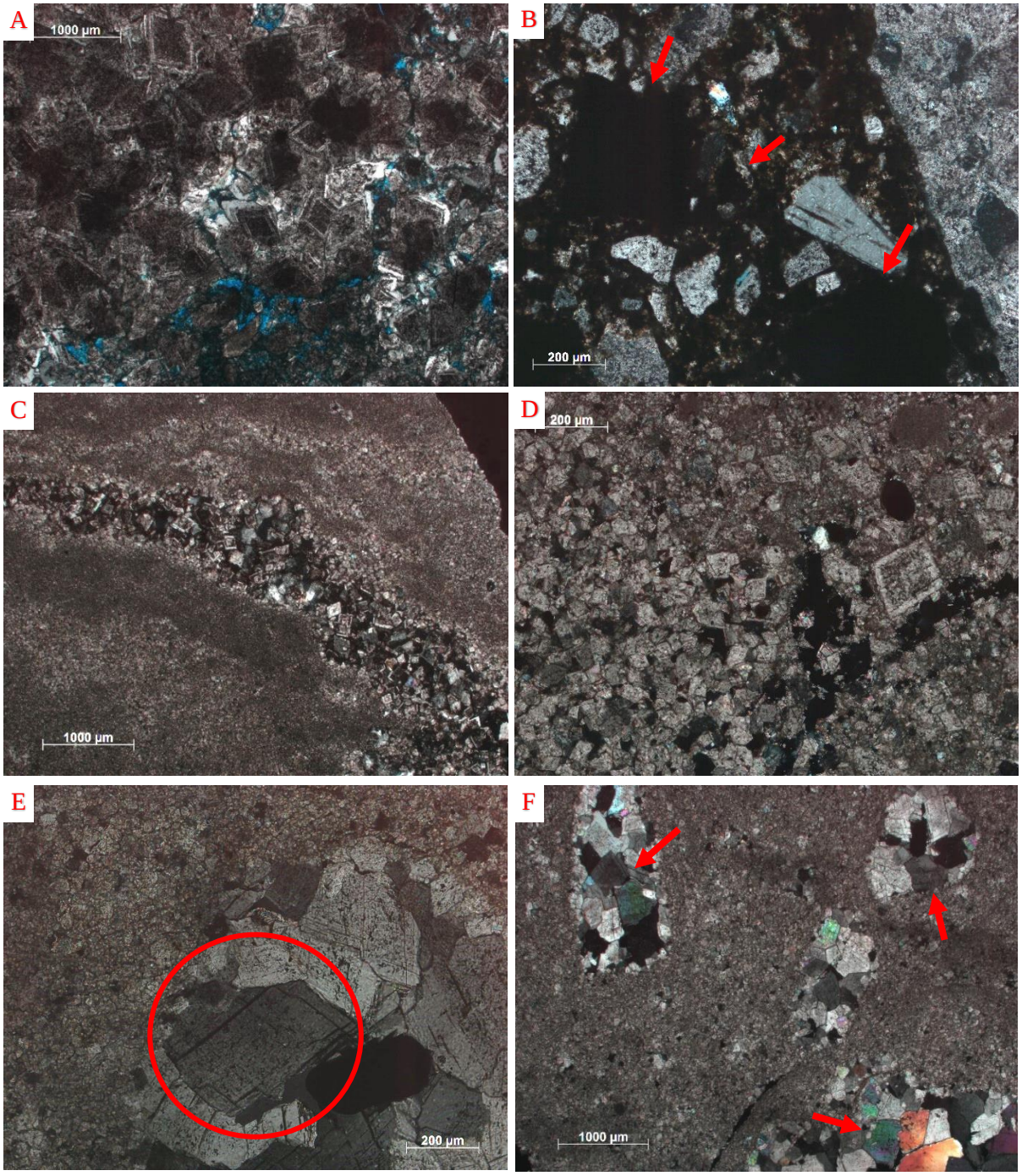


Figure 17: Photomicrographs in XPL (A) DVC 10-6B showing dolomite rhombs with dark/cloudy centers; (B) DVC 5-6 with opaque, cubic grains of galena and pyrite (arrows) and a clast of Jefferson City Dolomite on the right edge of the slide; (C) DV 17-1B Monomict breccia clasts with very fine grained dolomite but by a vein of larger dolomite rhombs that are being dedolomitized; (D) DV 8 showing dolomite rhombs with cloudy cores associated with opaque hematite grains; (E) DV 12-3 showing a close-up on a grain of baroque dolomite with curved grain boundaries and undulatory extinction; (F) DV 12-3 at lower magnification showing multiple vugs within the fine-grained matrix that contain baroque dolomite grains (arrows).

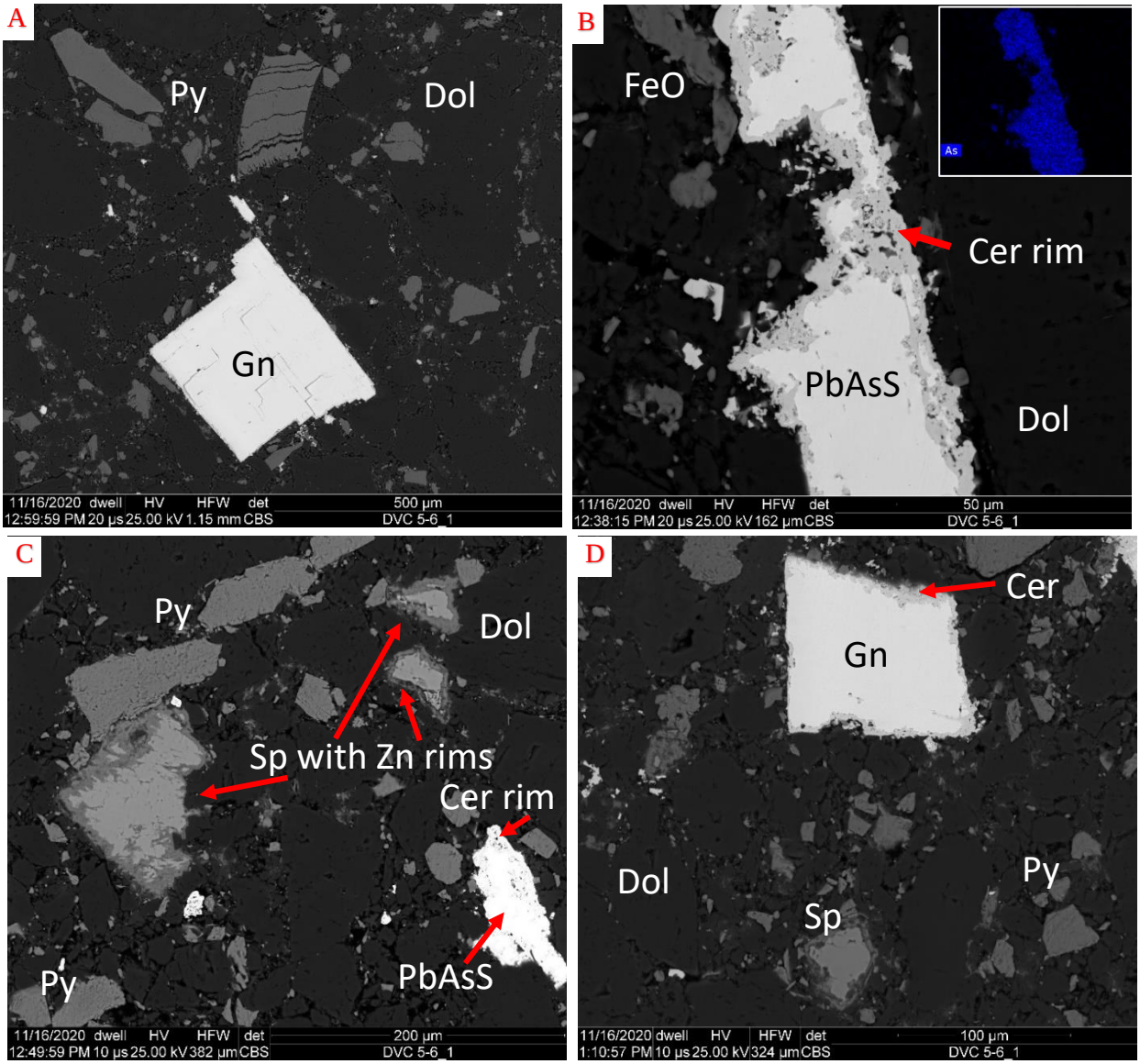


Figure 18: Backscatter SEM images (A) DVC 5-6 showing a large cube of galena, with pyrite and dolomite in the matrix; (B) DVC 5-6 showing the PbAsS mineral (possibly Jordanite, or galena with As inclusions) with inset map of As; (C) Another view of DVC 5-6 showing the PbAsS mineral with a similar fabric as seen in (B), pyrite is common in this sample and sphalerite is also abundant and contains pure zinc rims. The Pb rim on the PbAsS mineral is more difficult to see here because of the brightness, however it is still present; (D) This image shows a galena grain with a lead rim, similar to the lead rim seen on the PbAsS grain in (B) and is indicative of possible remobilization of sulfides during or shortly after impact.

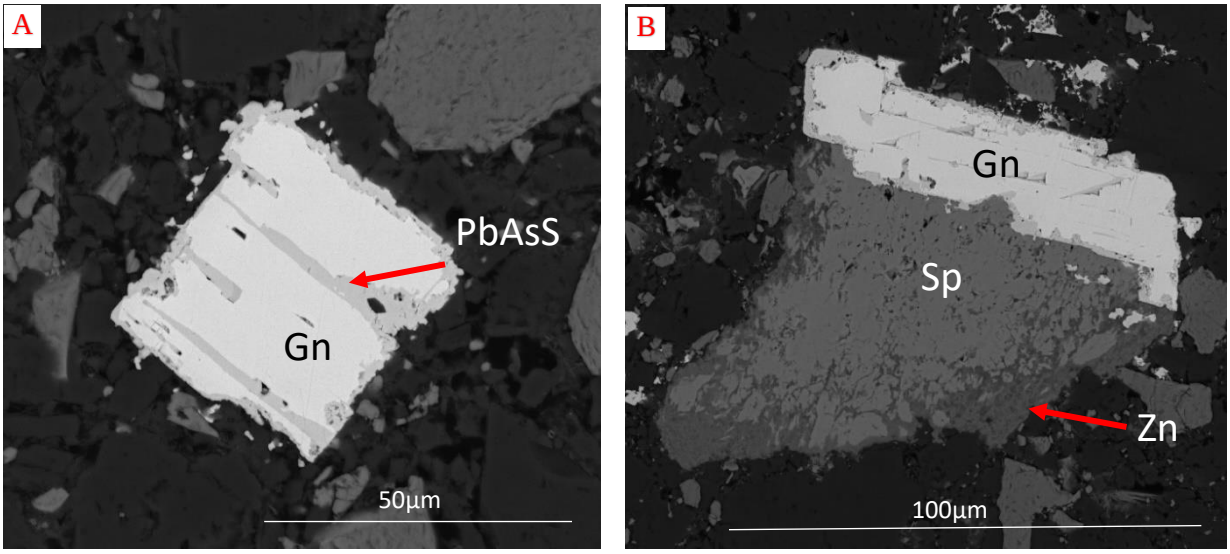


Figure 19: Backscatter SEM images of DVC 5-6 (A) contains a galena grain with As-inclusions along growth plains; (B) shows an intergrowth of galena and sphalerite which accounts for ~9% of the sulfides present in Decaturville (Zimmerman and Amstutz, 1972). The sphalerite here has a post-depositional zinc rim.

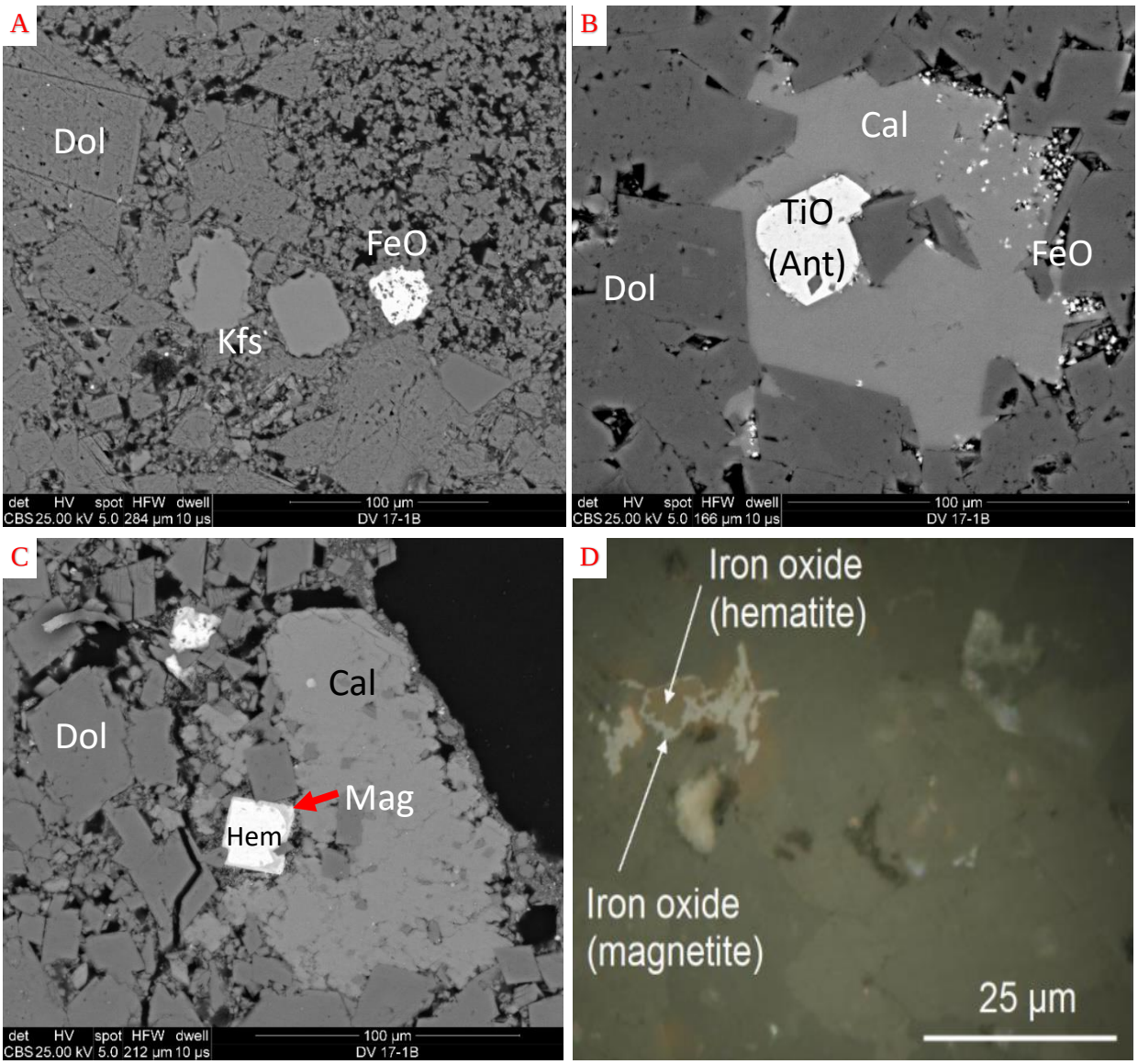


Figure 20: Backscatter SEM images (A) DV 8 containing mostly dolomite with K-feldspar and hematite; (B) DV 17-1B with calcite and hematite replacing dolomite, and a grain of authigenic anatase (C) DV 8 showing a pyrite cube that was entirely replaced by hematite, which was then partially replaced by magnetite; (D) Reflected light image of DV 17-1B showing further evidence of hematite being altered/replaced by magnetite (Dulin, 2006)

Diagenetic Phases	Relative timing Early	Middle	Late
Dolomite	----------		
Sphalerite	----------		
Galena	----------		
Pyrite (cubic)	----------		
Quartz	----------	----------	
K-feldspar		----------	----------
Hematite (replacing pyrite)		----------	
Anatase		----------	
Dedolomite (Hematite + Calcite)		----------	
Porosity/vug formation		----------	
Baroque dolomite		----------	----------
Galena with As inclusions			----------
Dissolution of Sphalerite (Zn rims)			----------
Dissolution of PbAsS (cerussite rims)			----------
Magnetite			----------

Figure 21: Paragenetic sequence for the Decaturville impact structure showing the relative timing of formation of authigenic phases. Highlighted green indicates pre-impact and yellow indicates post-impact (or impact related). The diagenetic phases in grey are those that are possibly impact-related but could also have formed pre-impact.

7. Isotope Results

A plot of the carbon and oxygen isotopic data can be seen in Figure 22. This shows the samples from Decaturville in blue triangles, Serpent Mound in purple diamonds, and Jeptha Knob in green squares. These values represent bulk samples, as micro-sampling was not possible. The range in values for δ13C is -2.6‰ to 3.6‰. The samples from Decaturville and Jeptha Knob are Ordovician in age and as can be seen in Figure 23, the values obtained for the carbon isotope ratios match with what is expected of typical marine carbonates during this time which have values around -2‰ to 0‰. The samples from Serpent Mound are Silurian in age and again the values obtained for the carbonates there match with what is shown in Figure 23 for typical marine carbonates during that time with values of approximately 0‰ to 6‰. The range for δ18O in these samples is -10.9‰ to -3.2‰. As can be seen in Figure 24, a plot of secular changes in δ18O, the typical range of δ18O values for marine limestones in the Ordovician-Silurian is -11‰ to -3‰ which matches what is observed in the samples from Jeptha Knob, Serpent Mound and Decaturville. There was also a pervious analysis of Sr isotopes done at Decaturville which found that the rocks are depleted in ^{87}Sr relative to ^{86}Sr and indicates the fluids were not externally-derived (Dulin, 2006).

It is thought that all carbonates as old as the ones discussed here have likely had their oxygen isotopic values altered due to reequilibration with meteoric water. The carbon isotope values of the samples discussed here are similar to marine carbonates for the appropriate age of the samples. This could indicate that, despite the likelihood of post depositional alteration of the oxygen values via meteoric water, the carbon values show little evidence of alteration by impact-generated hydrothermal fluids and this is consistent with the Sr isotope data discussed for Decaturville. As micro-sampling was unable to be performed, it was not possible to distinguish the values for the detrital phases from the different authigenic phases. As a result, it is difficult to make any definitive interpretations about the isotope results.

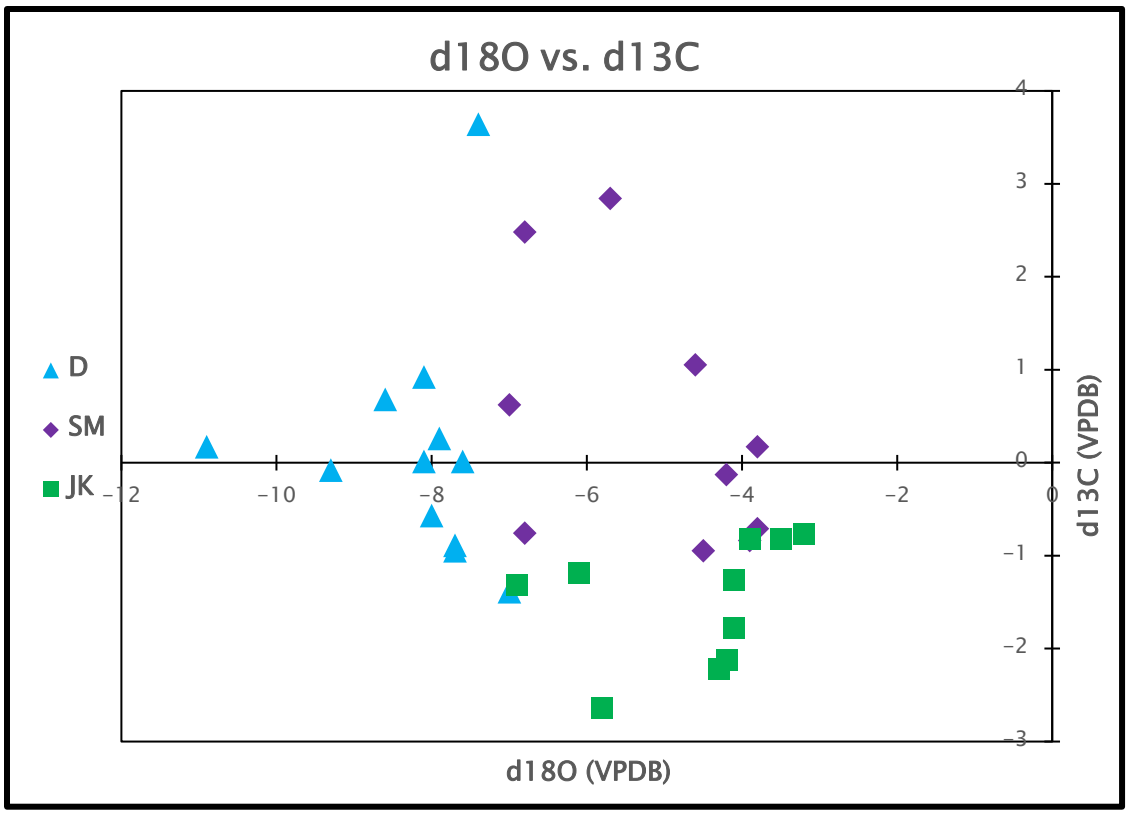


Figure 22: Plot of d18O on the x-axis vs. d13C on the y axis for all three structures. Decaturville (D) is shown in blue triangles, Serpent Mound (SM) is shown in purple diamonds, and Jeptha Knob (JK) is shown in green squares.

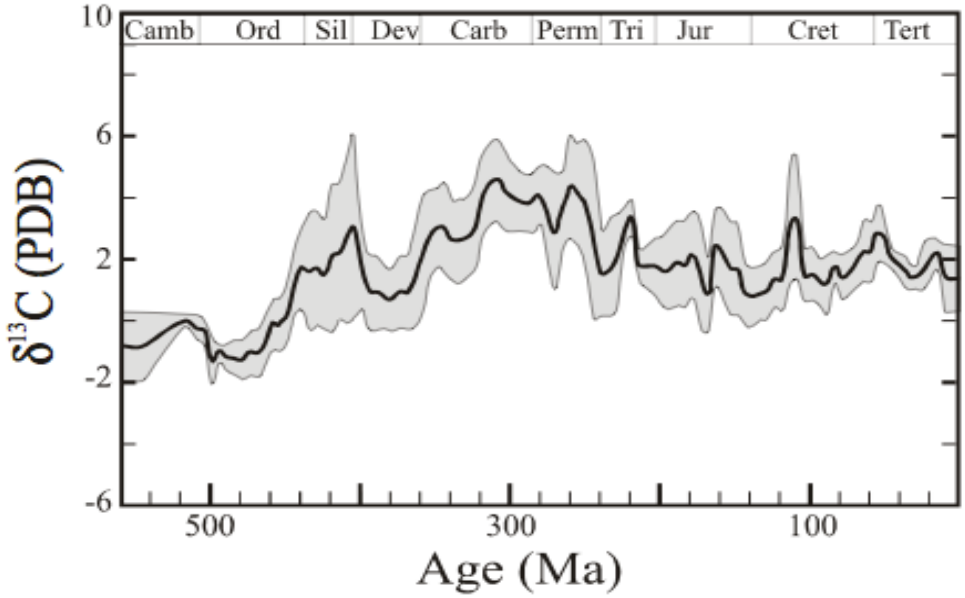


Figure 23: Plot showing the secular variations of d13C in marine carbonates with the shaded area showing the error. From (Veizer et al., 1999).

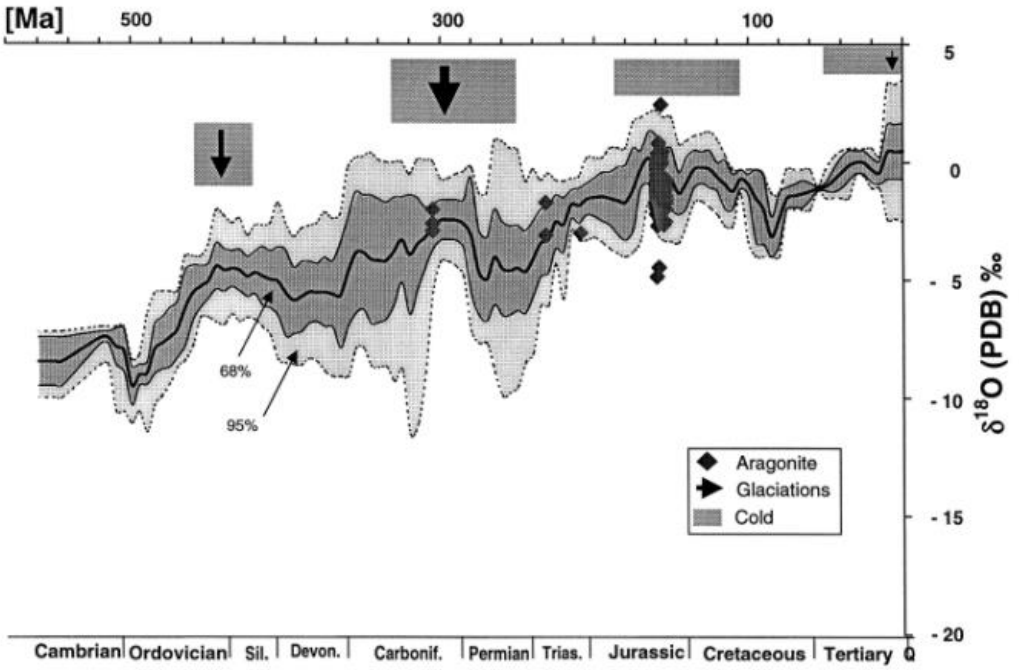


Figure 24: Plot showing the secular variations of d18O in marine carbonates with the shaded area showing the error. From (Veizer et al., 1999).

8. Discussion

8.1 Comparison with other hydrothermal systems

Impact-Related Alteration

Hydrothermal activity following impact has been identified in over half of all impact structures on Earth with diameters ranging in size from 1.8km (Lonar Lake) to 250km (Sudbury) (Osinski et al., 2012). As evidenced in the results sections, at all three structures discussed here there are phases present that are commonly found in complex impact structures that have experienced hydrothermal activity related to impact (e.g., Osinski et al., 2012). These phases include quartz, anatase, K-feldspar, biotite, and remobilized sulfides. It should be noted as discussed below, however, that these phases can form by mechanisms other than hydrothermal fluids. Figure 1 shows the 6 localities within complex impact structures where hydrothermal deposits are expected (Osinski et al., 2012). These locations include: 1) impact melt rocks and breccias that contain melt; 2) central uplifts; 3) transitional areas; 4) ejecta outside of the crater; 5) collapsed rim areas; and 6) post-impact sediments in instances where crater lakes form (Osinski et al., 2012). In the three structures presented in this paper there is evidence for hydrothermal deposits in localities 2, 3, and 5.

Previously, it was thought that impact melt is uncommon in impacts with carbonate target rocks because carbonates, when experiencing high pressures and temperatures, were thought to devolatilize more readily than silicates and experience decomposition rather than melting (O-Keefe and Ahrens, 1989). More recently it has been found that decomposition and devolatilization are limited and where they have been recognized are potentially related to contact metamorphic processes which occurred post-impact (Osinski et al., 2008). Impact melting is not uncommon and is now thought to be a dominant process occurring in carbonates (as well as crystalline rocks). However, because of textural and chemical differences, carbonate melt is difficult to recognize (Osinski et al., 2008). Evidence of melt-bearing breccias is present at both Serpent Mound and Decaturville (Baranoski et al., 2003; Beauford, 2012). At Serpent Mound, the potentially melt-bearing breccias are all located deep in the subsurface and were not sampled nor will they be discussed here. There is a lack of any breccias, or impact melt found at the surface at Serpent Mound because of the degree of erosion that has removed any ejecta material that had been present following impact (Baranoski et al., 2003). At Decaturville, impact melt-bearing breccias have been

identified due to macroscopic flow features (Beauford, 2012). Impact melted carbonates recrystallize as carbonates and generally do not contain many distinguishable features from unmelted carbonates, which is why identifying them has been so difficult in the past (Beauford, 2012). Evidence of hydrothermal activity was also found at Decaturville in location 1 (impact breccias).

The evidence of hydrothermal activity found in this study at location 1 (the impact breccias) at the Decaturville structure include remobilized sulfides, and baroque dolomite filling vugs (Figs. 16 and 15f, respectively). This is consistent with what is reported at the Haughton and Ries impact structures where hydrothermal mineralization within cavities, vugs, and fractures is common in impact breccias (Osinski et al., 2004 and Osinski et al., 2005), however the extent of hydrothermal mineralization in the matrix of these Decaturville breccias is much less than at the larger Haughton and Ries craters.

Evidence for hydrothermal activity at location 2 (central peaks; Figure 1) is present at all three structures examined in this study. This is generally in the form of authigenic quartz and anatase found in pore space and fractures (Figs. 8b, 12b), sulfides (Figs. 7b, 18), and calcite infilling veins/fractures (Fig. 11b). Again, this is consistent with what has been found in other impact structures where hydrothermal mineralization within the central peak area is typically isolated to vugs and veins. At Haughton impact structure, for example, abundant hydrothermal quartz is present in the central uplift (Osinski et al., 2012). Quartz, anatase, and calcite infilling vugs and veins are also common features identified relatively close to the central area of the Chicxulub structure (Zurcher and Kring, 2004).

At location 3 (crater floor/transition area) similar hydrothermal phases are found as at location 2 and these again include quartz and anatase, as well as K-feldspar (Figs. 8c, 12c), clays (Figs. 8a, 12c), biotite (Fig. 8c), and baroque dolomite (Fig. 6c). These are typically found infilling porosity and fractures which is common in other complex impact structures (Osinski et al., 2012). Some of these phases, specifically baroque dolomite and veins containing calcite, clays, and quartz, are consistent with what has been identified in the Kentland impact structure (Hamilton, 2019). At less eroded/ fresher craters these features are not found at the surface, as they are buried below crater-fill (melt rocks and breccias) like at the Haughton structure (Osinski et al., 2012).

Lastly, location 5 (crater rim) is the other location that all three of these structures have evidence of hydrothermal activity. The hydrothermal phases found close to the crater rims include baroque dolomite (Figs. 17e and f), K-feldspar (Fig. 20a), clays, quartz, and sulfides (specifically marcasite needles growing on pyrite cubes) (Fig. 12a). The presence of these phases near the rims of these three structures is also consistent with what has been found at Ries crater and Chicxulub (Osinski et al., 2005; Zurcher and Kring, 2004).

While hydrothermal phases are well documented at the surface in complex impact structures as a result of the conditions experienced during impact, there are also instances where there is little evidence of a hydrothermal system activated despite the size and environment of impact. Two structures with similar size and target material to Serpent Mound, Decaturville, and Jeptha Knob that show limited evidence of hydrothermal activity at the surface are the Flynn and Wells Creek structures in Tennessee.

Flynn Creek is an ~3.8km diameter complex impact structure containing deformed Ordovician through Devonian dolostones and limestones as well as an impact breccia unit (Roddy, 1968). It is confirmed as an impact structure by the presence of shatter cones, planar deformation features in quartz grains, and the remains of an ejecta layer (Roddy, 1968). Based on the stratigraphy present (limestone and dolostone) the depositional environment prior to and during impact was likely shallow marine. It's formation as a complex impact structure into a shallow marine setting indicates that the size and environmental setting of the Flynn Creek structure would have had the proper inputs to generate a hydrothermal system. Impact breccias in surface exposures were petrographically characterized by Rohleder (2019) and no hydrothermal phases were found. The main diagenetic phases present were dolomite, pyrite, iron oxides, and clays and these were not interpreted to have had a hydrothermal origin (Rohleder, 2019). In cores drilled into the structure, however, there does appear to be some evidence of a low-temperature (~97-125°) hydrothermal system (Gullikson et al., 2017). This includes hydrothermal fluorite, barite, calcite, K-feldspar, pyrite, and wollastonite found at ~500m depth below the central uplift and the transitional area (Gullikson et al., 2017; Gaither et al., 2017). The presence of hydrothermal deposits at depth, but not in the impact breccias at the surface could be the result of later hydrothermal fluids moving through fractures created at depth during the impact, but not an

impact-generated hydrothermal system. These could be orogenic fluids migrating through at the time of the Alleghany orogeny in the late Paleozoic.

The Wells Creek structure is a highly eroded impact structure and is larger than Flynn Creek at 12km in diameter. It contains deformed units ranging in age from Devonian to Mississippian that are composed of limestones and dolostones (Wilson and Stearns, 1968). It is confirmed as an impact structure based on the presence of shatter cones and impact breccias (Wilson and Stearns, 1968). Similar to Flynn Creek, the presence of limestones and dolostones indicates that the depositional environment was shallow marine, where water was available to generate a hydrothermal system during the impact event. No evidence of hydrothermal mineralization was found in samples collected near the rim of Wells Creek and the diagenetic phases only include dolomite, pyrite, and iron oxides (Rohleder, 2019). Wells Creek is listed as having evidence of hydrothermal activity in Osinski et al.'s (2012) paper, however the exact phases or the extent of this evidence is not discussed.

Based on what is observed at these other, well documented, impact structures, it is possible, and common, for a hydrothermal system to be generated during an impact event that is large enough to produce a complex impact structure. While this is the case, Flynn Creek and Wells Creek provide two examples where there likely was not impact-related hydrothermal activity. Because of the similar sizes and target lithologies present at the three structures focused on here to what is observed at Flynn and Wells creek, it is possible that the observed hydrothermal phases at Jeptha Knob, Serpent Mound, and Decaturville are not related to impact, although as evidenced above, it is also possible that they are related to impact. The phases may not be diagnostic of hydrothermal alteration via impact and could be related to hydrothermal orogenic fluid migration through the target rocks either prior to impact, or later through conduits opened during impact.

Non-Impact-Related Alteration

Hydrothermal fluid migration is a common occurrence on Earth and is not constrained to meteorite impact locations. There are many examples of locations with hydrothermal deposits that are related to orogenic fluids or igneous activity. Orogenic fluids are tectonic brines that are commonly released during convergent orogenic activity (Oliver, 1992) like the Appalachian-Ouachita-Marathon thrust belt in the United States. These fluids commonly propagate heat, fluids, and organic material through the country rock via interactions with groundwater and lead to the

formation of diagenetic phases and economic deposits (Bethke and Marashak, 1990). The Woodford shale in Oklahoma is an important source rock and unconventional reservoir for oil and gas production across the state. A diagenetic study of this unit in southeast Oklahoma found evidence of hydrothermal mineralization in fractures (Roberts and Elmore, 2018). The fractures formed during the Ouachita orogeny (in the late Paleozoic) when faulting occurred in southern Oklahoma and led to deformation in the units present, including the Woodford, which is cross-cut by faults (Roberts and Elmore, 2018). Mississippi Valley type lead zinc deposits are common throughout the central and eastern United States and are interpreted to have formed via fluid expulsions from foreland basins during this same event (Shelton et al., 1986). Concurrently with the deformation and Mississippi Valley type deposition, Ba-rich adularia (hydrothermal K-feldspar) was also formed in the Ouachita mountains as a result of the hot, high pressured fluids released during the Ouachita faulting (Shelton et al., 1986).

The hydrothermal assemblage in the Woodford shale includes baroque dolomite, magnesite, norsethite, witherite, gorceixite, K-feldspar, sphalerite, chalcopyrite, apatite, and albite, which were thought to have formed during middle-late diagenesis (Roberts and Elmore, 2018). Some of these phases are consistent with what was found at Jeptha Knob, Serpent Mound, and Decaturville including the baroque dolomite, K-feldspar, sphalerite, and apatite. This indicates that tectonic-related hydrothermal systems can produce similar hydrothermal assemblages to what is found in potentially impact-related hydrothermal settings. The presence of other hydrothermal phases in the Woodford shale like magnesite, norsethite, witherite, and gorceixite, which were not present in the impact structures presented here, could be related to the rock-type present (the difference in the available ions for mineralization in the shale versus in carbonates) and tectonic setting. This could also be the result of hydrothermal mineralization from externally derived fluids which would introduce other ions to the system that would allow for the formation of these other minerals in an open system (Roberts and Elmore, 2018). In impact-generated hydrothermal systems the fluids are likely not externally derived, as the heat input and deformation are all localized to the area directly surrounding the impact and would not allow for fluids that originated elsewhere to migrate into the system.

Other evidence of non-impact related hydrothermal systems producing similar phases to what was presented here is structurally controlled hydrothermal dolomite reservoirs. This is

important facies to understand for oil exploration specifically in the Michigan and Appalachian basins, as well as other basins in the eastern part of Canada and the US (Davies and Smith, 2006). Common features in these reservoirs are baroque dolomite, and vug-filling dolomite, as well as Mississippi Valley type sulfide deposits (Davies and Smith, 2006). These hydrothermal deposits appear to be structurally controlled by extensional faults where fluid flow is focused in the hanging wall (Davies and Smith, 2006). The source of the saline and Mg-rich fluids that lead to the formation of these hydrothermal dolomite reservoirs is unknown and more work needs to be done to understand them (Davies and Smith, 2006). However, they are very clearly not impact-related hydrothermal fluids. Pb and Zn mineralization, similar to what was discussed at Decaturville (Pb-Zn rims) has also been found in carbonate rocks that have not experienced impact (Lee and Wilkinson, 2002). In carbonate breccias from the Cooleen zone in Ireland, hydrothermal sulfide mineralization is thought to have occurred in a sea-floor environment where hydrothermal fluids dolomitized existing breccias and then sulfides replaced some of the dolomite (Lee and Wilkinson, 2002).

There are many other examples of hydrothermal mineralization that is not associated with an impact structure. In the examples discussed above it is clear that all the phases found at Jeptha Knob, Serpent Mound, and Decaturville are not innate to impact-generated hydrothermal systems and are able to be formed under non-catastrophic conditions commonly experienced on Earth. This makes it difficult to distinguish between impact-generated and non-impact-related diagenetic and hydrothermal events, specifically where the age of the hydrothermal phases is unknown in relation to the impact.

8.2 Summary of hydrothermal evidence at impacts

The presence of baroque dolomite, anatase, quartz, monazite, K-feldspar, biotite, and remobilized sulfides all suggest that hydrothermal systems could have been present at some point in the history of these structures. As discussed previously, it is common during impact events for a hydrothermal system to be generated because of the high pressures and temperatures experienced during impact. The fact that all of the target rocks discussed in these structures are limestones and dolostones indicates that during the time of impact, all three of these structures were likely in marine settings, and when combined with the increased heat during impact there would have been the correct ingredients to generate hydrothermal systems leading to the paragenesis of the

hydrothermal mineral assemblages observed. However, as is also discussed above, similar hydrothermal mineral assemblages are common in rocks that have not experienced impact. Based on the evidence presented in this study at Jeptha Knob, Serpent Mound, and Decaturville, it is difficult to determine if the hydrothermal phases were formed as a result of impact, or if they formed due to later hydrothermal fluid migration. Impact-related diagenetic features cannot be distinguished from non-impact-related diagenetic phases and therefore hypothesis 1 is not supported by the results of this study. Hypothesis 2 though, is supported as evidence of hydrothermal mineralization was found within all three structures but was not found in the samples collected from outside of the structures.

As mentioned above, impact-generated hydrothermal systems likely do not allow for externally-derived fluids to enter the system because the deformation and heat is localized to the structure. This could provide support for the notion that the hydrothermal phases discussed in Jeptha Knob, Serpent Mound, and Decaturville were formed during impact, and not during later orogenic fluid migration through conduits opened during impact. This is because all of the phases present could have formed due to recrystallization and remobilization of the ions that were already present in the limestone and dolostone units. As discussed in the results, a previous analysis of Sr isotopes at Decaturville found that the rocks are depleted in ^{87}Sr relative to ^{86}Sr which is indicative of fluids that are not externally-derived (Dulin, 2006). There were also not any exotic hydrothermal phases identified which would have indicated an open system and migration of externally derived fluids that would have sourced ions that were not already present in the system. The carbon isotopic data discussed from all three structures is not indicative of hydrothermal alteration from externally-derived fluids and the oxygen isotopic data matches the values that is expected from meteoric fluid interactions for carbonates of this age and is not indicative of impact-related hydrothermal alteration. However, because the longevity of an impact-generated hydrothermal system at craters of this size would likely not last very long, there may not have been time for isotopic reequilibration in the presence of impact-generated hydrothermal fluids, similar to what was discussed with the lack of hydrothermal alteration of the conodonts at Decaturville.

Based on what is presented here, the size of the impactor and the resultant impact structure likely plays a vital role in the extent of hydrothermal mineralization that is expected and also on the longevity of hydrothermal circulation. All three structures discussed here are relatively small

complex impact structures with diameters likely less than 10km. It was found that at Chicxulub (a 180km diameter structure) the temporal scale of hydrothermal activity was at least 300,000 years following impact into a marine setting (Rowe et al., 2004). Similar hydrothermal evidence has been identified at Chicxulub to what was discussed at the three structures presented here, though evidence of a more intense, long-lasting hydrothermal system is lacking at these three structures. This likely is a result of the higher energy influx from an impactor large enough to create a 180km diameter structure than what would be experienced during an impact resulting in a <10km diameter structure. The temporal scale of the hydrothermal system will be much longer in larger craters and lead to a more extensive hydrothermal assemblage.

7.3 Link to Paleomagnetic studies

As mentioned in the results sections for Serpent Mound and Decaturville, there were previous paleomagnetic studies on both impacts. At Serpent Mound this indicated that the hematite-rich section of the Brassfield formation has a magnetic age of Late Permian/ Early Triassic (Watts, 2004). This is an interesting issue because the dominant occurrence of hematite in these rocks is in the form of replaced allochems and hematite ooids that are determined to be predepositional and should have an Early Silurian age. The Late Permian/ Early Triassic age was interpreted to be due to the regional remagnetization event that effected much of the North American craton during the Kiaman reversed epoch (Watts, 2004). It is possible that the dedolomite and associated hematite identified in these rocks could be the explanation for the magnetization. If this is the case, then the dedolomitization may have formed during the periodic evaporitic conditions that Ohio was experiencing in the Permian. The regional remagnetization that likely overprinted any earlier magnetization is troubling as it makes paleomagnetic dating of earlier events difficult and due in part to this, the exact timing of the formation of Serpent Mound (and the hydrothermal phases present within) is unknown, though based on calcite twin orientations the lower age estimate is 290Ma (Schedl, 2006). This regional remagnetization also effected the Flynn and Wells Creek structures in Tennessee (Rohleder, 2019). Because of the proximity of Flynn and Wells Creek to Serpent Mound, it is highly likely that the Jeptha Knob structure (Kentucky) would also have been remagnetized due to this event, though because of COVID-19, samples were unable to be collected for paleomagnetic analysis in this thesis.

At Decaturville the previous paleomagnetic study found that the breccias from the southern outcrop contain a chemical remanent magnetization (CRM) in magnetite (Elmore and Dulin, 2007). As previously discussed, the magnetite is clearly authigenic and is found replacing hematite and pyrite. It was previously interpreted to have formed at low temperatures indicating it is not related to impact. This is because of the combination of the conodonts indicating low temperatures (<100°C) and the non-radiogenic Sr isotopic signatures (Elmore and Dulin, 2007). However, as discussed above, the hydrothermal activity associated with impact may not have been long-lived enough to alter the conodonts and based on the identification of baroque dolomite in vugs within the matrix of the breccias, there is evidence of moderate-high temperature fluids migrating through these rocks likely directly following impact. The lack of radiogenic Sr isotopic signatures is indicative of an internal fluid source (which would be likely during an impact generated hydrothermal system) without abundant feldspar present (which could increase the $^{87}Sr/^{86}Sr$ ratio). This indicates that the age of the CRM found (Permian) could be reinterpreted thanks to the new petrographic evidence to be possibly dating the impact as the magnetization could be related to the impact and not a later remagnetization as previously interpreted. In any case, the age of the CRM constrains the impact to pre-Permian.

This project helped to further our understanding of the hydrothermal influence in impact craters on Earth, which is important because hydrothermal settings are known to harbor life (e.g. Martin et al., 2008; Zierenberg et al., 2000). It is possible that, because hydrothermal systems helped to develop life on Earth, other bodies in our solar system, Mars specifically, could have had periodic life in the past thanks to impact-generated hydrothermal systems. During the Late Heavy Bombardment (~3.8Ga) our solar system experienced an increased flux of impactors. The earliest time period on Mars is called the Noachian and spanned the time of the Late Heavy Bombardment. During this time, the surface of Mars was dominated by phyllosilicates, indicating alteration by nonacidic waters (Bibring et al., 2006). Because of the likelihood for liquid water to have been present on Mars either at the surface, or in the shallow subsurface, it is possible that the conditions during impact would have allowed for hydrothermal systems to be generated. Impact-generated hydrothermal systems as a possible environment for the creation and sustenance of life on Mars was first suggested by Newsom et al (1986). Because of the abundance of impacts occurring and the increased likelihood for life to form in hydrothermal environments (e.g. Martin et al., 2008; Zierenberg et al., 2000), it is likely that if evidence of life is present on Mars, it will be found

within impact crater deposits. With the recent launch of the Mars Perseverance Rover, which has the goal to find signs of biosignatures in the rocks that formed on ancient Mars and a landing site into Jezero crater, this may be our best opportunity yet to find evidence of life on Mars related to an impact-generated hydrothermal system.

9. Conclusions

Of the two hypotheses that were tested in this study: 1. Impact related hydrothermal alteration can be distinguished from other non-impact-related diagenetic events, and 2. The alteration observed will be localized to the impact structure and not found in the country rock outside of the structures, only the second is supported by the results discussed here.

From what was found in Jeptha Knob, Serpent Mound, and Decaturville, impact related diagenesis, and impact-related hydrothermal alteration are not distinguishable from non-impact related events. This shows a lack of support for hypotheses 1 related to differentiating impact-related diagenesis and post-impact hydrothermal alteration from non-impact-generated events. There were no diagnostic phases identified that have not also been found at locations that experienced regular tectonic processes and not impact of an extraterrestrial object. This could be, in part, due to the target lithologies, degree of erosion, and size of the impact structures discussed here.

Hypothesis two, however is supported by the results as there is certainly evidence of hydrothermal alteration localized within all three of the structures, though this cannot be definitively stated as being related to impact and further work will need to be done to either confirm or deny this statement. That could include further paleomagnetic analysis, however as evidenced by the previous paleomagnetic studies done at Decaturville and Serpent Mound, there appears to have been later remagnetization/diagenesis that could have overprinted the exact timing of formation of the phases.

10. References:

Arp, G., Kolepka, C., Simon, K., Karius, V., Nolte, N. And Hansen, B.T., 2013, New evidence for persisten impact-generated hydrothermal activity in the Miocene Ries impact structure, Germany: Meteoritics and Planetary Science, v. 48, p. 2491-2516.

Baranoski, M. T., Schumacher, G. A., Watts, D. R., Carlton, R. W., and El-Saiti, B. M., 2003, Subsurface geology of the Serpent Mound disturbance, Adams, Highland, and Pike counties, Ohio: Ohio Division of Geological Survey Report of Investigation No. 146, 71 p.

Beauford, R. E., 2012, Carbonate melts and sedimentary impactite variation at Crooked Creek and Decaturville impact craters, Missouri, USA, Houston, Texas, Lunar and Planetary Institute, 43rd Lunar and Planetary Science Conference, abstract 1705.

Bell, M.S., Horz, F., and Reid, A., 1998, Characterization of experimental shock effects in calcite and dolomite by X-ray diffraction: Abstract of the Lunar and Planetary Science Conference XXIX, Lunar and Planetary science Institute, Houston, Texas

Bethke, C. M., and Marshak, S., 1990, Brine migrations across North America- the plate tectonics of ground water: Earth and Planetary Science, v. 18, p. 287-315.

Bibring, J.P., Langevin, Y., Mustard, J. F., Poulet, F., Arvidson, R., Gendrin, A., Gondet, B., Mangold, N., Pinet, P., Forget, F., and the OMEGA team, 2006, Global mineralogical and aqueous Mars history derived from OMEGA/Mars Express data: Science, v. 312, p. 400-404.

Borella, P. E., and Osborne, R. H., 1978, Late Middle and early Late Ordovician history of the Cincinnati arch province, central Kentucky to central Tennessee: Geological Society of American Bulletin, v. 89, p. 1559-1573.

Botoman, G., and Stieglitz, R. D., 1978, The occurrence of sulfide and associated minerals in Ohio: Ohio Department of Natural Resources Report of Investigations No. 104, 16 p.

Brett, C. E., Goodman, W. M., and LoDuca, S. T., 1990, Sequences, cycles, and basin dynamics in the Silurian of the Appalachian Foreland Basin: Sedimentary Geology, v. 69, p. 191-244.

Burkhard, M., 1993, Calcite twins, their geometry, appearance and significance as stress-strain markers and indicators of tectonic regime: a review: Journal of Structural Geology, v. 15, no. 3-5, p. 351-368.

Butler, I. B., and Rickard, D., 2000, Framboidal pyrite formation via the oxidation of iron monosulfide by hydrogen sulphide: Geochemica et Cosmochimica Acta, v. 64, p. 2665-2672.

Clarke, F.W., Washington, H.S., 1924, The composition of the Earth's crust: Washington government printing office, professional paper 127.

Cressman, E. R., 1981, Surface geology of the Jeptha Knob cryptoexplosion structure, Shelby County, Kentucky: Geological Survey Professional Paper 1151-B.

Davies, G. R., and Smith, L. B., 2006, Structurally controlled hydrothermal dolomite reservoir facies: an overview: AAPG Bulletin, v. 90, no. 11, p 1641-1690.

Di Bella, C., Sabatino, G., Quartieri, S., Ferretti, A., Cavalazzi, B., Barbieri, R., Foucher, F., Messori, F., and Italiano, F., 2019, Modern iron ooids of hydrothermal origin as a proxy for ancient deposits: Nature Scientific Reports, 9:7107.

Dietz, R.S., 1960, Meteorite impact suggested by shatter cones in rock: Science, v. 131, no. 3416, p. 1781-1784.

Dulin, S.A. and Elmore, R.D., 2008, Paleomagnetism of the Weaubleau structure, southwestern Missouri: The Geological Society of America Special paper 437.

Dulin, S.A., Elmore, R.D., Dennie, D.P., Evans, S.C., and Mulvany, P., 2007, Paleomagnetic investigations of the Decaturville, MO and Sierra Madera, TX impact structures: 42nd Lunar and Planetary Science Conference Abstract 1120.

Dulin, S. A., 2006, Paleomagnetic investigation of impacts in carbonate target rocks, [Master's Thesis]: University of Oklahoma, 69 p.

Elmore, R. D., Dunn, W., and Peck , C., 1985, Absolute dating of dedolomitization by means of paleomagnetic techniques: Geology, v. 13, p, 558-561.

Elmore, R. D., and Dulin, S.A., 2007, New paleomagnetic age constraints on the Decaturville impact structure and Weaubleau structure along the 38th parallel in Missouri (North America): Geophysical Research Letters, v. 34.

Elmore, R. D., Muxworthy, A. R., and Aldana, M., 2012, Remagnetization and chemical alteration of sedimentary rocks: Geological Society, Longdon, Special Publications, no. 371, p. 1-21.

Fox, M. E., 2014, An Assessment of shock metamorphism for Jeptha Knob, A suspected impact crater in North-Central Kentucky [Master's thesis]: Ohio University, 263 p.

French B. M., 1998, Traces of Catastrophe: A Handbook of Shock-Metamorphic Effects in Terrestrial Meteorite Impact Structures: LPI Contribution No. 954, Lunar and Planetary Institute, Houston. 120 pp.

Gaither, T. A., Hagarty, J. J., Villareal, K. A., Gullikson, A. L., and Leonard, H., 2017, Flynn Creek impact crater: petrographic and SEM analyses of drill cores from the central uplift, Houston, Texas, Lunar and Planetary Institute, Lunar and Planetary Science XLVIII, abstract 2263.

Gillhaus, A., Richter, D. K., Gotte, T., and Neuser, R. D., 2010, From tabular to rhombohedral dolomite crystals in Zechstein 2 dolostones from Scharzfeld (SW Harz/Germany): A case study with combined CL and EBSD investigations: Sedimentary Geology, v. 228, p. 284-291.

Grieve, R. A. F., 2005, Economic natural resource deposits at terrestrial impact structures *in* Mcdonald, I., Boyce, A. J., Butler, I. B., Herrington, R. J., and Polya, D. A., 2005, Mineral Deposits and Earth Evolution: Geological society of London, special publications, v. 248, p. 1-29.

Grieve, R. A. F., and Masaitis, V. L., 2010, The economic potential of terrestrial impact craters: International Geology Review, v. 36, p. 105-151.

Gullikson, A. L., Gaither, T. A., Villarreal, K. A., and Hagarty, J. J., 2017, Petrographic characterization and preliminary microthermometry of the hydrothermal system at Flynn Creek crater, Tennessee, 8th Planetary Crater Consortium, abstract 1718.

Hamilton, C., 2019, A paleomagnetic and diagenetic study of the Kentland impact crater [Master's thesis]: University of Oklahoma, 64 p.

Hanss, R. E., Montague, B. R., Davis, M. K., Galindo, C., and Horz, F., 1978, X-ray diffractometer studies of shocked materials: Proc. Lunar Planet. Scie Conf. 9th, p. 2773-2787.

Hecht, L., Freiberger, R., Gilg, H. A., Grundmann, G., Kostitsyn, Y. A., 1998, Rare earth element and isotope (C, O, Sr) characteristics of hydrothermal carbonates: genetic implications for dolomite-hosted talc mineralization at Gopfersgrun (Fichtelgebirge, Germany): Chemical Geology, v. 155, p. 115-130.

Heyl, A.V., and Brock, M. R., 1962, Zinc occurrence in the serpent Mound structure of southern Ohio: US Geological Survey Professional Paper 450-D, p. D95-D97.

Hudson, J. D., 1977, Stable isotopes and limestone lithification: Journal of the Geological Society of London, v. 133, p. 637-660.

Hull, D., Bacon, D.J., 2001, Introduction to dislocations: Butterworth-Heinemann Publications. 5th edition. 257 pp.

Kahle, C, 1988, Surface and subsurface paleokarst, Silurian Lockport, and Peebles Dolomites, Wester Ohio, *in* James, N.P, and Choquette, P.W., Paleokarst: Springer-Verlag New York Inc., p. 229-240.

Kyser, T. K., James, N. P., and Bone, Y., 2002, Shallow burial dolomitization and dedolomitization of Cenozoic cool-water limestones, southern Australia: geochemistry and origin: Journal of Sedimentary Research, v. 72, no. 1, p. 146-157.

Langenhorst, F., 2002, Shock metamorphism of some minerals: Basic introduction and microstructural observations: Bulletin of the Czech Geologic Survey, v. 77, no. 4, p. 265-282.

Leach, D. L., Taylor, R. D., Fey, D. L., and Diehl, S. F., 2010, A deposit model for Mississippi Valley-Tyle lead-zinc ores: US Geological Survey Scientific Investigations Report 2010-5070-A.

Lee, M. J., and Wilkinson, J. J., 2002, Cementation, hydrothermal alteration and Zn-Pb mineralization of carbonate breccias in the Irish midlands: textural evidence from the Cooleen zone, near Silvermines, County Tipperary: Economic Geology, v. 97, p. 653-662.

Loucks, V. and Elmore, R. Douglas, 1986, Absolute dating of dedolomitization and the origin of magnetization in the Morgan Creek Limestone, central Texas: GSA Bull., v. 97, p. 486-496.

Martin, W. D., 1998, Geology of the Dunkard group (upper Pennsylvanian-Lower Permian) in Ohio, West Virginia, and Pennsylvania: Ohio Division of Geological Survey Bulletin 73.

Martin, W., Baross, J., Kelley, D., and Russell, M. J., 2008, Hydrothermal vents and the origin of life: Nature Reviews Microbiology, v. 6, p. 805-814.

Martinez, I., Agrinier, P., Scharer, U., and Javoy, M., 1994, A SEM-AETM and stable isotope study of carbonates from the Haughton impact crater, Canada: Earth and Planetary Science Letter, v. 121, p. 559-574.

McCabe, C., and Elmore, R. D., 1989, The occurrence and origin of Late Paleozoic remagnetization in the sedimentary rocks of North America: Reviews Of Geophysics, v. 2, p. 471-494.

Melosh, H.J., 1989, Impact Cratering: A Geologic Process: New York, Oxford University Press, 245p.

Milam, K. A., 2010, A revised diameter for the Serpent Mound impact crater in Southern Ohio: Ohio Journal of Science, v. 110, p. 34-43.

Milam, K., Hester, A., and Malinksi, P., 2010, An anomalous breccia associated with the Serpent Mound impact crater, Southern Ohio: Ohio Journal of Science, v. 110 p. 18-30.

Montañez, I.P., 1997, Secondary porosity and late diagenetic cements of the upper Knox group, Central Tennessee region: a temporal and spatial history of fluid flow conduit development within the Knox regional aquifer in Basin-Wide Diagenetic Patterns: Integrated Petrologic, Geochemical, and Hydrologic Considerations: GeoScienceWorld Books.

Murowchick, J. B., and Barnes, H. L., 1987, Effects of temperature and degree of supersaturation on pyrite morphology: American Mineralogist, v. 72, p. 1241-1250.

Newsom, H. E., Graup, G., Sewards, T., and Keil, K., 1986, Fluidization and hydrothermal alteration of the suevite deposit in the Ries crater, West Germany, and implications for Mars: Journal of Geophysical Research, v. 91, p. 239-251.

Oakley, L. M., 2013, Enhanced resolution of the paleoenvironmental and diagenetic features of the Silurian Brassfield Formation [Master's thesis] Wright State University, 116 p.

Offield, T.W., Pohn, H.A., 1979, Geology of the Decaturville impact structure, Missouri: U.S. Geological Survey Professional Paper 1042.

O-Keefe, J. D., and Ahrens, T. J., 1989, Impact production of CO_2 by the Cretaceous/Tertiary extinction bolide and the resultant heating of the Earth: Nature, v. 338, p. 247-249.

Oliver, J., 1992, The spots and stains of plate tectonics: Earth-Science Reviews, v. 32, p. 77-106.

Osinski G. R., Spray, J. G., and Grieve, R. A. F., 2008, Impact melting in sedimentary target rocks: an assessment: The geological Society of America Special Paper 437.

Osinski, G. R., Grieve, R. A. F., and Spray, J. G., 2004, The nature of the groundmass of surficial suevites from the Ries impact structure, Germany, and constraints on its origin: Meteoritics and Planetary Science, v. 39, p. 1655-1684.

Osinski, G. R., Lee, P., Parnell, J., Spray, J. G., and Baron, M., 2005, A case study of impact-induced hydrothermal activity: the Haughton impact structure, Devon Island, Canadian High Arctic: Meteoritics and Planetary Science, v. 40, p. 1859-1878.

Osinski, G.R., Tornabene, L.L., Banerjee, N.R.,, Cockell, C.S., Flemming, R., Izawa, M.R.M., McCutcheon, J., Parnell, J., Preston, L.J., Pickersgill, A.E., Pontefract, A., Sapers, H.M, and Southam, G, 2012, Impact-generated hydrothermal systems on Earth and Mars: Icarus, c. 224, p. 347-363.

Overstreet, W. C., 1967, The geologic occurrence of monazite: Geological Survey Professional Paper 530.

Pirajno, F., 1992, Hydrothermal mineral deposits – principles and fundamental concepts for the exploration geologists. Springer-Verlag, Berlin, Heidelberg.

Reidel, S. P., 1972, Geology of Serpent Mound cryptoexplosion structure [Master's thesis]: University of Cincinnati, 150 p.

Reidel, S. P., Koucky, F. L., and Stryker, J. R., 1982, The Serpent Mound disturbance, southwestern Ohio: American Journal of Science, v. 282, p. 1343-1377.

Roberts, J. M., and Elmore, R. D., 2018, A diagenetic study of the Woodford Shale in the southeastern Anadarko Basin, Oklahoma, USA: Evidence for hydrothermal alteration in mineralized fractures: Interpretation, v. 6, p. SC1-SC13.

Roddy, D.J., 1968. The Flynn Creek Crater, Tennessee. In: French, B.V., Short, N.M. (Eds), Shock Metamorphism of Natural Materials, Mono Book Corp., Baltimore, 291–322.

Rohleder, N., 2019, Paleomagnetic analysis of the Flynn Creek and Welss Creek impact structures, Tennessee, U.S.A. [Master's Thesis]: University of Oklahoma 67 p.

Rowe, A. J., Wilkinson, J. J., Coles, B. J., and Morgan, J. V., 2004, Chicxulub: Testing for post-impact hydrothermal input into the Tertiary ocean: Meteoritics and Planetary Science, v. 39, p. 1223-1231.

Schedl, A. D., 2006, Applications of twin analysis to studying meteorite impact structures: Earth and Planetary science letters, v. 244, p. 530-540.

Schedl, A. D., and Seabolt, A., 2016, The challenges of studying meteorite impacts into carbonate rocks: Jeptha Knob Kentucky, Houston, Texas, Lunar and Planetary Institute, 47th Lunar and Planetary Science Conference, abstract 1589.

Scholle, P. A., and Ulmer-Scholle, D. A., 2003, A color guide to the petrography of carbonate rocks: grains, textures, porosity, diagenesis: AAPG Memoir 77.

Seeger, C.R., 1968, Origin of the Jeptha Knob structure Kentucky: American Journal of Science, v. 266, p. 630-660.

Shelton, K. L., Reader, J. M., Ross, L. M., and Viele, G. W., 1986, Ba-rich adularia from the Ouachita Mountains, Arkansas: Implications for a postcollisional hydrothermal system: American Mineralogist, v. 71, p. 916-923.

Simpson, E. N., 2019, The effect of sample processing on X-ray diffraction peaks of dolomite: Implications for studies of shock metamorphosed materials [Bachelor's thesis] Ohio University, 44 p.

Skala, R., Matejka, P., Ederova, J., and Horz, F., 2000, Mineralogical investigations of experimentally shocked dolomite: implications for the outgassing of carbonates: Geological Society of America Special Papers, v. 2002, no. 356, p. 571-585.

Spangenberg, J., Fontbote, L., Shapr, Z.D., and Hunziker, J., 1996, Carbon and oxygen isotope study of hydrothermal carbonates in the zinc-lead deposits of the San Vicente district, central Peru: a quantitative modeling on mixing processes and CO2 degassing: Chemical Geology, v. 133, p. 289-315.

Vanadia, D. S., 2017, Mapping the outer margin of the Spernt Mound impact structure to assess the outer limit of deformation: Adams, Highland, and Pike Counties, Ohio [Master's thesis] Ohio University, 91 p.

Varga, L. L., 1981, Dolomitization of the Brassfield Formation (lower Silurian) in Adams, County, Ohio [Master's thesis] Western Michigan University, 85 p.

Veizer, J., Ala, D., Azmy, K., Bruckschen, P., Buhl, D., Bruhn, F., Carden, G. A. F., Deiner, A., Ebneth, S., Godderis, Y., Jasper, T., Korte, C., Pawallek, F., Podlaha, O. G., and Strauss, H., 1999, $^{87}Sr/^{86}Sr$, $\delta 13C$ and $\delta 18O$ evolution of Phanerozoic seawater: Chemical Geology, v. 161, p. 59-88.

Von Morlot, 1847 as cited by Schoenherr, J., Reunig, L., Hallenberger, M., Luders, V., Lemmens, L., Biehl, B. C., Lewin, A., Leupold, M., Wimmers, K., and Strohmenger, C. J., 2018, Dedolomitization: review and case study of uncommon mesogenetic formation conditions: Earth-Science Reviews, v. 185, p. 780, 805.

Warren, J., 2000, Dolomite: occurrence, evolution and economically important associations: Earth-Science Reviews, v. 52, p. 1-81.

Watts, D.R., 2004, Paleomagnetic determination of the age of the Serpent Mound structure: The Ohio Journal of Science, v. 104, no. 4, p. 101-108.

Waugh, B., 1978, Authigenic K-feldspar in British Permo-Triassic sandstones: Journal of the Geological Society of London, v. 135, p. 51-56.

Wilshire, H.G., Howard, K.A., and Offield, T.W., 1971, Impact breccias in carbonate rocks, Sierra Madera, Texas: Geological Society of America Bulletin, v. 82, no. 4, p. 1009-1018.

Wilson, C. W., and Stearns, R. G., 1968, Geology of the Wells Creek structure, Tennessee: Tennessee Division Geology Bulletin 68.

Young, T. P., 1989, Phanerozoic ironstones: an introduction and review in Young, T. P. and Taylor, W. E. G., 1989, Phanerozoic Ironstones, Geological Society Special Publication, n0. 46, p. ix-xxv.

Zheng, Y. F., and Hoefs, J., 1992, Carbon and oxygen isotopic covariations in hydrothermal calcites: Mineralium Deposita, v. 28, p. 79-89.

Zierenberg, R. A., Adams. M. W. W., and Arp, A. J, 2000, Life in extreme environments: Hydrothermal vents: Proceedings of the National Academy of Sciences, v. 97, p. 12961-12962.

Zimmerman, R. A., and Amstutz, G. C., 1972, Intergrowth and crystallization features in the Cambrian mud volcanoe of Decaturville, Missouri, U.S.A in Amstutz, G. C., and Bernard, A. J., Ores in Sediments: VIII. International Sedimentological Congress, Heidelberg.

Zurcher, L. and Kring, D.A., 2004, Hydrothermal alteration in the core of the Yaxcopoil-1 borehole, Chicxulub impact structure, Mexico: Meteoritics and Planetary Science, v. 39, no. 4, p. 1199-1221.